



## Calhoun: The NPS Institutional Archive

---

Theses and Dissertations

Thesis Collection

---

2008-06

# Dynamic simulation of particles in a magnetorheological fluid

Spinks, Joseph Michael.

Monterey California. Naval Postgraduate School

---



Calhoun is a project of the Dudley Knox Library at NPS, furthering the precepts and goals of open government and government transparency. All information contained herein has been approved for release by the NPS Public Affairs Officer.

**Dudley Knox Library / Naval Postgraduate School**  
**411 Dyer Road / 1 University Circle**  
**Monterey, California USA 93943**

<http://www.nps.edu/library>



# **NAVAL POSTGRADUATE SCHOOL**

**MONTEREY, CALIFORNIA**

## **THESIS**

### **DYNAMIC SIMULATION OF PARTICLES IN A MAGNETORHEOLOGICAL FLUID**

by

Joseph M. Spinks

June 2008

Thesis Advisor:

John Lloyd

**Approved for public release; distribution is unlimited**

THIS PAGE INTENTIONALLY LEFT BLANK

<b>REPORT DOCUMENTATION PAGE</b>			<i>Form Approved OMB No. 0704-0188</i>	
Public reporting burden for this collection of information is estimated to average 1 hour per response, including the time for reviewing instruction, searching existing data sources, gathering and maintaining the data needed, and completing and reviewing the collection of information. Send comments regarding this burden estimate or any other aspect of this collection of information, including suggestions for reducing this burden, to Washington headquarters Services, Directorate for Information Operations and Reports, 1215 Jefferson Davis Highway, Suite 1204, Arlington, VA 22202-4302, and to the Office of Management and Budget, Paperwork Reduction Project (0704-0188) Washington DC 20503.				
<b>1. AGENCY USE ONLY (Leave blank)</b>		<b>2. REPORT DATE</b> June 2008	<b>3. REPORT TYPE AND DATES COVERED</b> Master's Thesis	
<b>4. TITLE AND SUBTITLE</b> Dynamic Simulation of Particles in a Magnetorheological Fluid			<b>5. FUNDING NUMBERS</b>	
<b>6. AUTHOR(S)</b> Joseph M. Spinks				
<b>7. PERFORMING ORGANIZATION NAME(S) AND ADDRESS(ES)</b> Naval Postgraduate School Monterey, CA 93943-5000			<b>8. PERFORMING ORGANIZATION REPORT NUMBER</b>	
<b>9. SPONSORING /MONITORING AGENCY NAME(S) AND ADDRESS(ES)</b> N/A			<b>10. SPONSORING/MONITORING AGENCY REPORT NUMBER</b>	
<b>11. SUPPLEMENTARY NOTES</b> The views expressed in this thesis are those of the author and do not reflect the official policy or position of the Department of Defense or the U.S. Government.				
<b>12a. DISTRIBUTION / AVAILABILITY STATEMENT</b> Approved for public release; distribution is unlimited			<b>12b. DISTRIBUTION CODE A</b>	
<b>13. ABSTRACT (maximum 200 words)</b> <p>The mechanical and rheological properties of a MR fluid depend on the induced microstructure of the imbedded ferrous particles. When subject to an external field these particles magnetize and align themselves in chains parallel to the applied magnetic field. The microstructure of these chains is a function of several parameters including particle size, applied magnetic field strength, and viscosity and velocity of the surrounding fluid. This thesis will create a model from a first principle approach to accurately predict the microstructure in a variety of different situations. The model investigated assumes the particles become magnetic dipoles upon the application of the magnetic field and that particle interaction is due solely to dipole-dipole interaction. Due to the inherently small size of the particles, drag is modeled using Stokes' drag. This mathematical model will be used to create a computer simulation to visualize and analyze the subsequent transient microstructures formed. The model will assume a constant magnetic field applied (IE no spatial or time gradients) and that the effects of this field are felt instantaneously.</p>				
<b>14. SUBJECT TERMS</b> Magnetorheological Fluid, Smart Fluid, Magnetic Dipole Interaction, Electrorheological Fluid			<b>15. NUMBER OF PAGES</b> 81	
			<b>16. PRICE CODE</b>	
<b>17. SECURITY CLASSIFICATION OF REPORT</b> Unclassified	<b>18. SECURITY CLASSIFICATION OF THIS PAGE</b> Unclassified	<b>19. SECURITY CLASSIFICATION OF ABSTRACT</b> Unclassified	<b>20. LIMITATION OF ABSTRACT</b> UU	

NSN 7540-01-280-5500

Standard Form 298 (Rev. 2-89)  
Prescribed by ANSI Std. Z39-18

THIS PAGE INTENTIONALLY LEFT BLANK

**Approved for public release; distribution is unlimited**

**DYNAMIC SIMULATION OF PARTICLES IN A MAGNETORHEOLOGICAL  
FLUID**

Joseph M. Spinks  
Lieutenant United States Navy  
B.S., University of Mississippi, 2001

Submitted in partial fulfillment of the  
requirements for the degree of

**MASTER OF SCIENCE IN MECHANICAL ENGINEERING**

from the

**NAVAL POSTGRADUATE SCHOOL  
June 2008**

Author: Joseph Michael Spinks

Approved by: John Lloyd  
Thesis Advisor

Anthony Healey  
Chairman, Department of Mechanical and Astronautical  
Engineering

THIS PAGE INTENTIONALLY LEFT BLANK

## **ABSTRACT**

The mechanical and rheological properties of an MR fluid depend on the induced microstructure of the imbedded ferrous particles. When subject to an externally applied magnetic field these particles magnetize and align themselves in chains parallel to the applied field. The microstructure of these chains is a function of several parameters including particle size, applied magnetic field strength, and viscosity and velocity of the surrounding fluid. This thesis will create a model from a first principle approach to accurately predict the microstructure in a variety of different situations. The model investigated assumes the particles become magnetic dipoles upon the application of the magnetic field and that particle interaction is due solely to dipole-dipole interaction. Due to the inherently small size of the particles, drag is modeled using Stokes' drag. This mathematical model will be used to create a computer simulation to visualize and analyze the subsequent transient microstructures formed. The model will assume a constant magnetic field applied (i.e., no spatial or time gradients) and that the effects of this field are felt instantaneously.



THIS PAGE INTENTIONALLY LEFT BLANK

## TABLE OF CONTENTS

<b>I.</b>	<b>INTRODUCTION</b>	<b>1</b>
<b>A.</b>	<b>CONTROLLABLE FLUIDS</b>	<b>1</b>
<b>B.</b>	<b>INDUSTRIAL APPLICATIONS</b>	<b>2</b>
<b>C.</b>	<b>TYPICAL MR FLUID ARRANGEMENT</b>	<b>3</b>
<b>II.</b>	<b>MAGNETIC FORCE</b>	<b>5</b>
<b>A.</b>	<b>DIPOLE MODEL</b>	<b>5</b>
<b>B.</b>	<b>FORCE ON A DIPOLE</b>	<b>6</b>
<b>III.</b>	<b>OTHER FORCES</b>	<b>11</b>
<b>A.</b>	<b>DRAG FORCE</b>	<b>11</b>
<b>B.</b>	<b>GRAVITY</b>	<b>11</b>
<b>C.</b>	<b>BROWNIAN MOTION</b>	<b>12</b>
<b>D.</b>	<b>REPULSIVE FORCES</b>	<b>12</b>
<b>E.</b>	<b>INTERACTION WITH ELECTROMAGNET</b>	<b>14</b>
<b>IV.</b>	<b>MODEL FOR INTERACTION</b>	<b>17</b>
<b>A.</b>	<b>NEWTON'S SECOND LAW</b>	<b>17</b>
<b>B.</b>	<b>STATIC FLUID MODEL</b>	<b>18</b>
<b>C.</b>	<b>DYNAMIC FLUID MODEL</b>	<b>19</b>
<b>V.</b>	<b>SIMULATION RESULTS</b>	<b>21</b>
<b>A.</b>	<b>STATIC FLUID SIMULATION</b>	<b>21</b>
<b>B.</b>	<b>DYNAMIC FLUID SIMULATION</b>	<b>43</b>
<b>VI.</b>	<b>CONCLUSION</b>	<b>47</b>
	<b>APPENDIX A. DERIVATIONS OF EQUATION 4, 5, AND 6</b>	<b>49</b>
	<b>APPENDIX B. COMPUTER CODE AND DESCRIPTION</b>	<b>53</b>
	<b>LIST OF REFERENCES</b>	<b>63</b>

THIS PAGE INTENTIONALLY LEFT BLANK

## LIST OF FIGURES

Figure 1.	MR Fluid Device Arrangement .....	3
Figure 2.	Dumbbell Shape.....	5
Figure 3.	Relationship Between Two Particles .....	8
Figure 4.	Simulation 1, Initial Particle Distribution, 3-D View .....	22
Figure 5.	Simulation 1, Initial Particle Distribution, Top Down View .....	22
Figure 6.	Simulation 1, Time = 0.16 milliseconds, 3-D View .....	23
Figure 7.	Simulation 1, Time = 0.16 milliseconds, Top Down View .....	23
Figure 8.	Simulation 1, Time = 1.7 milliseconds, 3-D View .....	24
Figure 9.	Simulation 1, Time = 1.7 milliseconds, Top Down View .....	24
Figure 10.	Simulation 2, Initial Particle Distribution, 3-D View .....	25
Figure 11.	Simulation 2, Initial Particle Distribution, Top Down View .....	25
Figure 12.	Simulation 2, Time = 0.16 milliseconds, 3-D View .....	26
Figure 13.	Simulation 2, Time = 0.16 milliseconds, Top Down View .....	26
Figure 14.	Simulation 2, Time = 0.86 milliseconds, 3-D View .....	27
Figure 15.	Simulation 2, Time = 0.86 milliseconds, Top Down View .....	27
Figure 16.	Simulation 2, Time = 1.7 milliseconds, 3-D View .....	28
Figure 17.	Simulation 2, Time = 1.7 milliseconds, Top Down View .....	28
Figure 18.	Simulation 3, Initial Particle Distribution, 3-D View .....	29
Figure 19.	Simulation 3, Initial Particle Distribution, Top Down View .....	29
Figure 20.	Simulation 3, Time = 0.16 milliseconds, 3-D View .....	30
Figure 21.	Simulation 3, Time = 0.16 milliseconds, Top Down View .....	30
Figure 22.	Simulation 3, Time = 0.86 milliseconds, 3-D View .....	31
Figure 23.	Simulation 3, Time = 0.86 milliseconds, Top Down View .....	31
Figure 24.	Simulation 3, Time = 1.7 milliseconds, 3-D View .....	32
Figure 25.	Simulation 3, Time = 1.7 milliseconds, Top Down View .....	32
Figure 26.	Simulation 4, Initial Particle Distribution, 3-D View .....	34
Figure 27.	Simulation 4, Initial Particle Distribution, Top Down View .....	34
Figure 28.	Simulation 4, Time = 0.86 milliseconds, 3-D View .....	35
Figure 29.	Simulation 4, Time = 0.86 milliseconds, Top Down View .....	35
Figure 30.	Simulation 4, Time = 1.7 milliseconds, 3-D View .....	36
Figure 31.	Simulation 4, Time = 1.7 milliseconds, Top Down View .....	36
Figure 32.	Simulation 5, Initial Particle Distribution, 3-D View .....	37
Figure 33.	Simulation 5, Initial Particle Distribution, Top Down View .....	37
Figure 34.	Simulation 5, Time = 0.86 milliseconds, 3-D View .....	38
Figure 35.	Simulation 5, Time = 0.86 milliseconds, Top Down View .....	38
Figure 36.	Simulation 5, Time = 1.7 milliseconds, 3-D View .....	39
Figure 37.	Simulation 5, Time = 1.7 milliseconds, 3-D View .....	39
Figure 38.	Simulation 6, Initial Particle Distribution, 3-D View .....	40
Figure 39.	Simulation 6, Initial Particle Distribution, Top Down View .....	40
Figure 40.	Simulation 6, Time = 0.86 milliseconds, 3-D View .....	41
Figure 41.	Simulation 6, Time = 0.86 milliseconds, Top Down View .....	41
Figure 42.	Simulation 6, Time = 1.7 milliseconds, 3-D view .....	42

Figure 43.	Simulation 6, Time = 1.7 milliseconds, Top Down View .....	42
Figure 44.	Side View of a MR Fluid in Shear.....	44
Figure 45.	Top View of the MR Fluid in Shear .....	45
Figure 46.	Side View of MR Fluid with Parabolic Flow .....	46
Figure 47.	Top Down View of MR Fluid with Parabolic Flow .....	46
Figure 48.	Geometrical Relationship Between Two Particles .....	49

## LIST OF TABLES

Table 1.	Parameters for Simulations 1, 2 and 3 .....	21
Table 2.	Parameters for Simulations 4, 5 and 6 .....	33
Table 3.	Parameters for Simulation 7.....	43

THIS PAGE INTENTIONALLY LEFT BLANK

## **ACKNOWLEDGMENTS**

I would like to thank my thesis advisor, Dr. John Lloyd, for his guidance and support during the thesis process. Without his help the completion of this thesis would not have been possible.

I would also like to thank Dr. James Luscombe for teaching me magnetic theory in a way that an engineering student could understand and use.



THIS PAGE INTENTIONALLY LEFT BLANK

# I. INTRODUCTION

## A. CONTROLLABLE FLUIDS

Magnetorheological (MR) and electrorheological (ER) fluids are a class of “smart” materials that are characterized by their ability to reversibly transform from liquid state to a Bingham solid. They are fluids that have either magnetically permeable (or electrically conductive) microscopic particles suspended in them. The transformation from liquid state to Bingham solid occurs by the application of a magnetic (or electric) field to the fluid. This magnetic (or electric) field causes the suspended particles to align in chains along the field lines in a manner to reduce the overall energy of the field. The existence of these chains changes many bulk properties of the fluid. Of practical interest is the change in viscosity which causes the fluid to behave like a Bingham solid.

The Bingham model used for modeling MR fluids relates the total shear stress  $\tau$  to the shear rate  $\dot{\gamma}$  and  $H$  (magnitude of applied magnetic field) according to the equation

$$\tau = \left[ \tau_y(H) + \eta \left| \dot{\gamma} \right| \right] \text{sgn}(\dot{\gamma}),$$

where  $\tau_y(H)$  is a yield stress that is a function of the applied magnetic field and  $\eta$  is the composite bulk viscosity of the fluid [1]. This equation is phenomenological in nature where the values in the equation are determined experimentally instead of being deduced from a first principle approach.

Recently it has been found that a more detailed approach to predicting the behavior of MR fluids has become necessary due to the limitations of the above approach [1]. First, the Bingham model is a macro scale approach (the fluid and particles are treated as a single continuum instead of a composite system) with no differentiation with particle level. The coupling between mechanical behavior and the magnetic field takes place at the particle level and is governed by first principles (conservation of momentum, Maxwell’s Laws, etc.). The Bingham model then is limited to a narrow range of

applicability commensurate with the experimental data. Second, the Bingham model tends to be inaccurate at low value of stress. In current applications where MR devices are used as feedback controls, low value stresses are important and the above model proves unsatisfactory. Third, the Bingham model is only applicable to 1-D simple shear flows with a transverse magnetic field applied. This is inadequate for multi-degree of freedom MR devices that are currently being designed. These reasons encourage a different model to be developed that is based on first principles.

## **B. INDUSTRIAL APPLICATIONS**

The American inventor, Willis Winslow, was the first to recognize how to create a smart fluid using these principles [2, 3]. He did much of the initial pioneering work on ER fluids in the 1940s. Later, Jacob Rabinow investigated the same phenomenon using a magnetic field for use in a magnetic field clutch [2] and is considered the first to develop MR fluids. Although their works were conducted over half a century ago, it has only been recently that the use of these smart fluids has become more common in industrial applications. This is due primarily to the stability and durability requirements of modern designs [3].

Today the uses for these smart, controllable fluids are numerous and varied. One primary use is in hydraulic dampers and brakes. Because of the ability to rapidly change the working fluid viscosity, one has the ability to change the damping coefficient in dampers to give much better dynamic response and control. Other applications include better feedback to control items such as joysticks, responsive personnel armor, and MR polishing machines [4].

### C. TYPICAL MR FLUID ARRANGEMENT

A typical arrangement for an industrial application of a MR fluid is shown below.

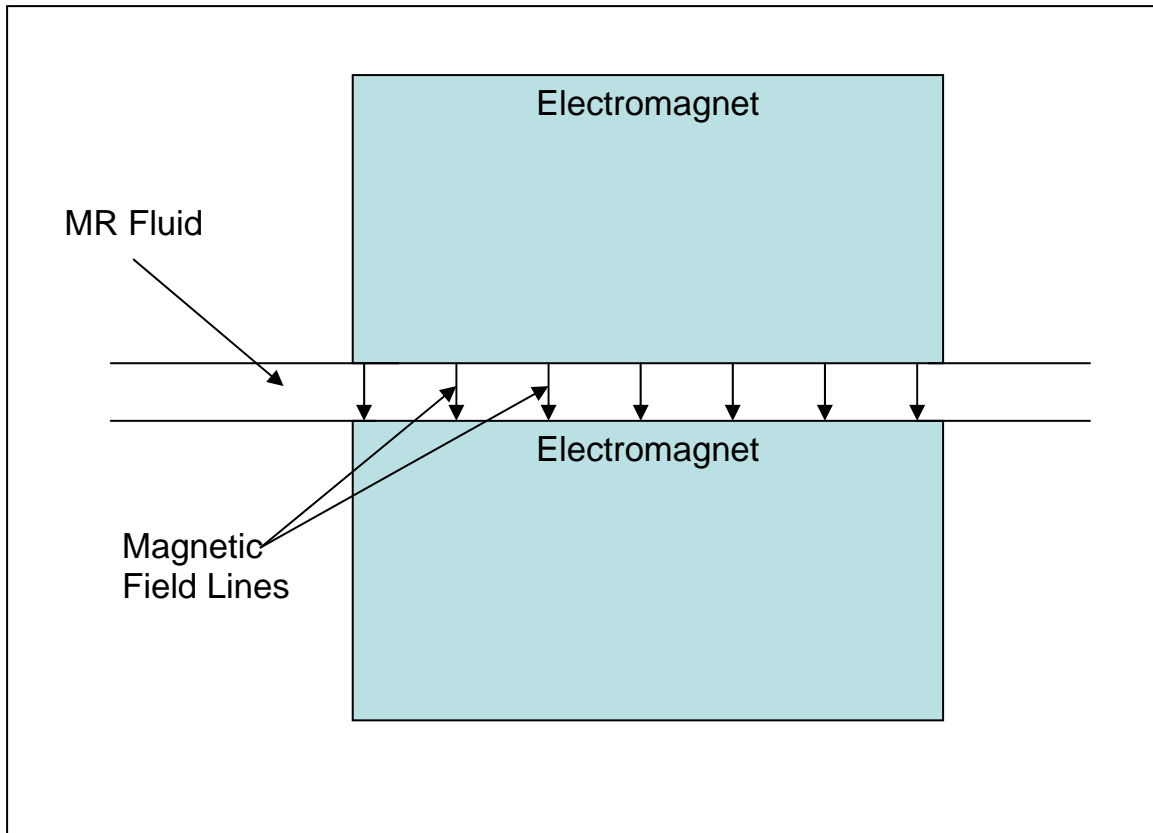


Figure 1. MR Fluid Device Arrangement

The MR fluid, consisting of a carrier fluid (usually a silicone oil) and the suspended particles (typically fine ferrous particles), is sandwiched in a small gap between two electromagnets. These magnets, when energized, create a magnetic field perpendicular to the flow of the MR fluid which causes the imbedded particles to form chains parallel to the applied field. The dynamic response of these particles in both a static fluid and a moving fluid is investigated in this thesis.

THIS PAGE INTENTIONALLY LEFT BLANK

## II. MAGNETIC FORCE

### A. DIPOLE MODEL

When the magnetic field is applied to the MR fluid, the ferromagnetic particles become magnetized and interact with the field and with each other. The exact solution to these interactions is difficult (if not impossible) and involves the integration of Maxwell's stress tensors across the entire volume of the magnetized solution. Instead, some simplifying assumptions need to be made in order to allow an easily calculable analytical solution without sacrificing accuracy.

The first assumption to be made is to use a dipole model for the magnetized particles. This assumes that the particles are dumbbell in shape, with length  $L$ . One end contains the positive (North) pole and the other contains the negative (South) pole of the magnet as shown in Figure 2. The magnitude of the pole strength is denoted by  $q$  and arises because the applied magnetic field magnetizes the particle.

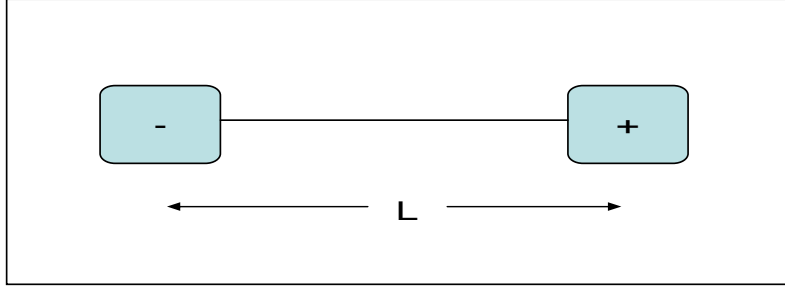


Figure 2. Dumbbell Shape

When the above dumbbell is placed in a magnetic field  $H$ , it experiences a torque about its center as described by the formula  $\tau = LqH \sin(\theta)$ , where  $\theta$  is the angle between the magnetic field and dumbbell. The quantity  $L*q$  is given a special name, the magnetic moment, and is denoted by  $m$ . The model used in this thesis uses the dipole model and is defined by determining the value of  $m$  in the limit where  $L$  goes to zero but the torque remains finite. This is the case of magnetic spheres which are used in most MR applications.

The magnitude of the dipole moment determines the interaction of the particles with the external magnetic field and the interaction of the particles with each other. It is a function of the magnitude of the applied external field ( $H$  with units Amp/m), the volume of the particles, and the magnetic permeability of both the particles and the surrounding fluid [5]. Specifically it is given by the relation

$$m = (4\pi a^3) \left( \frac{\mu_p - \mu_f}{\mu_p + 2\mu_f} \right) H_{loc} \quad (1)$$

where  $a$  = radius of the particle (meters),  $\mu_p$  = magnetic permeability of the particle (henry/meter),  $\mu_f$  = magnetic permeability of the fluid, and  $H_{loc}$  = magnetic field at dipole location (amp/meter).

Several assumptions need to be made when using the above formula. The presence of a dipole alters the magnetic field in its vicinity (this is what causes particles to interact with each other) and this implies that the value of  $H_{loc}$  needs to be calculated at every point. However, this variation is assumed to be negligible when calculating the magnetic dipole since the external fields applied are relatively large (on the order of 200 kA/m) and the variations caused by the dipoles are several orders of magnitude smaller. Therefore  $H_{loc}$  is assumed to be equal to the applied magnetic field. The second assumption concerns the value of  $\mu_p$ . Because the particles are ferrous,  $\mu_p$  is not a constant but varies with the applied magnetic field. However since the range of the applied field is small, often a fixed value, an average value of  $\mu_p$  is used based on the values of the applied field.

## B. FORCE ON A DIPOLE

The force on a dipole in a magnetic field is given by the product of the dipole moment and the gradient of the magnetic field as given by the expression

$$\vec{F}_r = m \frac{\partial \vec{H}}{\partial r} \quad (2)$$

where  $\vec{F}_r$  is the force in some arbitrary direction  $r$  and  $\frac{\partial \vec{H}}{\partial r}$  is the spatial derivative in the  $r$  direction. One method that presents itself in determining the forces is to simply calculate the magnetic field at every point. Theoretically this could be done by calculating the external applied field and modifying it by the perturbations caused by the presence of the dipoles. Since the location of the dipoles constantly changes, this calculation would have to be performed at every time step. Using this calculation (which would have to be performed numerically) the gradient at every point could be calculated and then the force on every particle could be determined. In reality this calculation is difficult to perform, requires specific algorithms for determining the field and the gradients, and requires massive computing power. A more simplistic approach was used for this model.

The first assumption for a more simplistic approach is that the applied magnetic field is uniform. This assumption is valid since the applied magnetic field is enacted rapidly (assumed instantaneous), does not vary with time, and the fluid gap is very small compared to the surface area over which the field is enacted. Since the magnetic field is assumed uniform in space and time there is no gradient and the particles experience no net force due to the external field. The only magnetic force the particles experience is due to their mutual interactions.

Consider two magnetic dipoles of identical strength at arbitrary positions  $\vec{r}_i$  and  $\vec{r}_j$ . A magnetic field  $\vec{H}_0$  is applied parallel to the  $z$  axis. The force between the two dipoles is given by

$$\vec{f}_{ij} = \frac{3m^2\mu_f}{r_{ij}^4} \left[ (1 - 3\cos^2 \theta_{ij}) \vec{e}_r - \sin(2\theta_{ij}) \vec{e}_\theta \right] \quad (3)$$

where  $\vec{f}_{ij}$  is the force on particle  $i$  from particle  $j$ ,  $r_{ij} = |\vec{r}_i - \vec{r}_j|$ ,  $\theta_{ij}$  is the angle from the  $z$  axis and  $\vec{r}_{ij}$ ,  $\vec{e}_r$  is a unit vector parallel to  $\vec{r}_{ij}$ , and  $\vec{e}_\theta$  is a unit vector parallel to  $\vec{e}_r \times (\vec{e}_r \times \vec{H}_0)$  [6]. This is shown in the below figure.



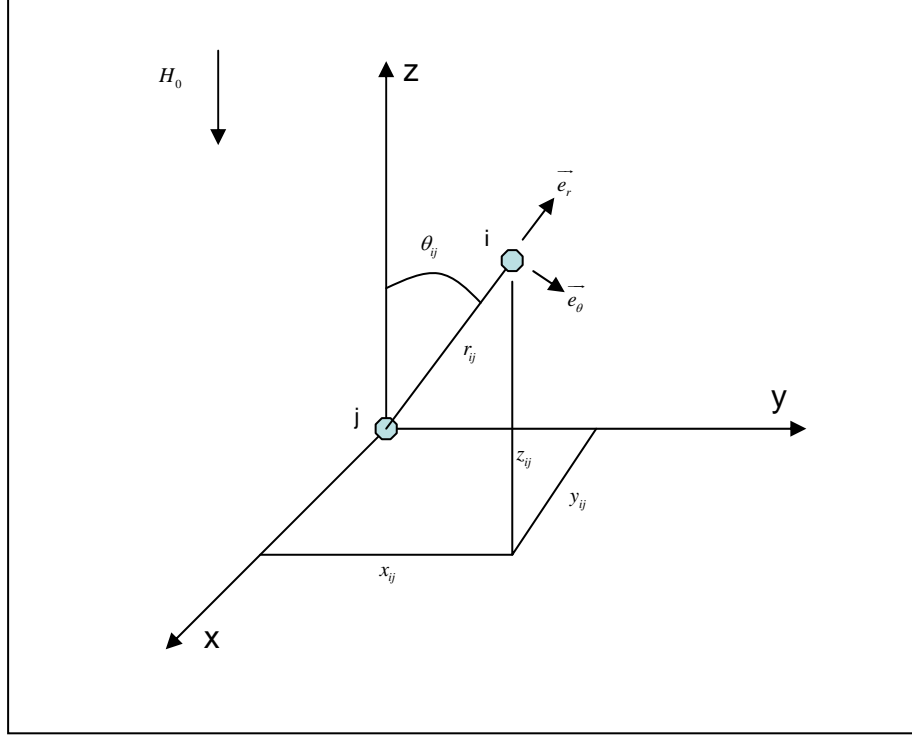


Figure 3. Relationship Between Two Particles

This equation models the interaction between dipoles and it is useful to examine this equation quantitatively to obtain a feel for the dynamics of the particles. By combining equations (1) and (2), it becomes apparent that the interaction force is proportional to the square of the applied field, proportional to the square of the particles volume, and the direction of the force is a function of the relative location of the two particles. This last item is what causes the particles to form stable chains when the magnetic field is applied. Examine only the radial term in equation (3). If  $\theta_{ij}$  is less than  $\sim 54.6$  degrees, the particles tend to attract. Otherwise they tend to repel.

It is more useful to transform equation (3) into Cartesian coordinates. Using the same x, y, and z directions as shown in Figure (2) and defining  $Q = 3m^2\mu_f$ , the x, y, and z components are given as

$$f_{ijx} = \frac{Q}{r_{ij}^4} \left[ 1 - \frac{5z_{ij}^2}{r_{ij}^2} \right] \frac{x_{ij}}{r_{ij}} \quad (4)$$

$$f_{ijy} = \frac{Q}{r_{ij}^4} \left[ 1 - \frac{5z_{ij}^2}{r_{ij}^2} \right] \frac{y_{ij}}{r_{ij}} \quad (5)$$

$$f_{ijz} = \frac{Q}{r_{ij}^4} \left[ 3 - \frac{5z_{ij}^2}{r_{ij}^2} \right] \frac{z_{ij}}{r_{ij}} \quad (6)$$

where  $f_{ijx}$  is the x component of  $f_{ij}$ ,  $f_{ijy}$  is the y component of  $f_{ij}$ , and  $f_{ijz}$  is the z component of  $f_{ij}$ . The derivations for the above equations are attached in Appendix A.

In a suspension of  $N$  particles each with an assumed induced magnetic dipole moment of  $m$ , the total magnetic force due to dipole interaction on a particle  $i$  is the sum of the contributions of all of the other particles in the suspension. In algebraic form

$$F_{Mix} = \sum_{i \neq j}^N f_{ijx} \quad (7)$$

$$F_{Miy} = \sum_{i \neq j}^N f_{ijy} \quad (8)$$

$$F_{Miz} = \sum_{i \neq j}^N f_{ijz} \quad (9)$$

where  $F_{Mix}$  is the total magnetic force on particle  $i$  in the x direction,  $F_{Miy}$  is the total magnetic force on particle  $i$  in the y direction, and  $F_{Miz}$  is the total magnetic force on particle  $i$  in the z direction. To determine the dynamic behavior of the particles in the fluid, these equation are calculated at every time step, the deviation in the current position of the particles are calculated, the values of the forces are recomputed at the next time step based on the particles' new position, and the process is repeated until the end of the computational time.

THIS PAGE INTENTIONALLY LEFT BLANK

### III. OTHER FORCES

#### A. DRAG FORCE

The drag force on a spherical particle moving in a viscous fluid is a function of the pressure difference across the sphere (form drag) and the surface shear stress (viscous drag). In general this expression can be complicated to solve. In the specific case of the small particles used in MR fluids a number of simplifying assumptions can be made to more easily determine this drag force. The flow can be assumed to be laminar due to the small clearances between the electromagnets which the fluid flows between and the small velocities analyzed in this thesis. Another simplifying case arises due to the small particle size ( $\sim$ micro meter) which implies that the Reynolds number based on diameter ( $Re_D$ ) is less than 1. Both of these assumptions allow the viscous drag force to be modeled by the well understood Stokes' drag which is given by

$$F_r = 6\pi\eta a \frac{dr}{dt} \quad (10)$$

where  $F_r$  is the drag force in the  $r$  direction,  $\eta$  is the viscosity of the fluid and  $a$  is the radius of the particle.

#### B. GRAVITY

The force of gravity is neglected in this model based on the fact that the gravitational force that would tend to make the particles settle is a much weaker force than the magnetic force that acts between the dipoles. This is obviously not true when no magnetic field is applied, but the gravitational settling is ignored by assuming that the suspension is thoroughly mixed before the application of the field and that the particles are randomly distributed in the carrier fluid.

### C. BROWNIAN MOTION

Brownian motion is characterized by the random walk of particles in a fluid due to the bombardment of molecules. In determining if Brownian motion should be considered in any model of MR fluids, this effect should be compared to other effects which determine the dynamic behavior of the particles. When there is no applied magnetic field this is not the case, however by assuming that the fluid is mixed immediately before the field is applied would negate any effects of Brownian motion. Once the field is applied the relative effect of Brownian motion compared with the magnetic forces can be determined by analyzing the coupling constant  $\lambda$  which is defined as the ratio of the interaction energy of two dipoles in contact and the thermal energy [6]. Specifically

$$\lambda = \frac{E_d}{k_b T} = \frac{\pi \mu_0 a^3 \chi^2 H^2}{9 k_b T} \quad (11)$$

where  $\mu_0$  is the magnetic permeability in a vacuum,  $a$  is the particle radius,  $H$  is the magnetic field,  $\chi$  is the magnetic susceptibility of the particle,  $k_b$  is the Boltzmann constant and  $T$  is the absolute temperature. In all cases modeled in this thesis  $\lambda \gg 1$  and Brownian motion is ignored.

### D. REPULSIVE FORCES

The particles themselves and any walls that physically constrain the MR fluid are modeled as hard surfaces. Therefore a fictitious repulsive force must be modeled to ensure that a particle in physical contact with either a wall or another particle behaves as hard. The characteristics of this force are such that when two particles touch (the distance between two dipoles is  $2a$  apart) the repulsive force exactly balances the attractive force between the dipoles, and when the distance between the dipoles is greater than  $2a$  the force is negligibly small. The proposed form of this force is given below

$$f_{rep,ij} = K_1 e^{K_2 \left[ \frac{r_{ij}}{2a} - 1 \right]} \mathbf{e}_r \quad (12)$$

where  $K_1$  and  $K_2$  are constants to be determined. The exponential term was chosen to give a function that rapidly decays as  $r_{ij}$  increases and is a commonly used mathematical model for these types of interactions [7].

To determine  $K_1$ , apply the condition that when  $r_{ij}$  is equal to  $2a$  then the repulsive force must equal the attractive force between the dipoles. From equation (3) the dipoles attract when  $\theta_{ij}$  is less than  $\sim 54.6$  degrees and the attractive force also causes  $\theta_{ij}$  to tend to zero. This is what causes the particles to align in chains that characterize the MR fluid. Assume that the particles will touch when  $\theta_{ij}$  is small. From Figure 2, this implies that  $x_{ij}$  and  $y_{ij}$  are negligibly small. Applying this condition to equations (4-6) gives

$$f_{ijx} = 0, f_{ijy} = 0, \text{ and } f_{ijz} = \frac{Q}{r_{ij}^4} \left[ 3 - \frac{5z_{ij}^2}{r_{ij}^2} \right] \frac{z_{ij}}{r_{ij}}.$$

When the particles are touching  $z_{ij} = r_{ij} = 2a$  which, when combined with the above equation, gives

$$f_{ijz} = -\frac{2Q}{(2a)^4}.$$

Combining this result with equation (9) gives a value for  $K_1 = \frac{Q}{8a^4}$ .

The constant  $K_2$  is determined by a much less rigorous means. It must be negative to give a decaying characteristic and its magnitude is selected by a trial and error approach. On one hand a high magnitude gives a steeper decay which is advantageous since this more closely approximates reality. However, if the value is too large, the repulsive term can become extremely large for small distances and leads to numerical instabilities. A value of  $K_2 = -12$  was chosen as a balance between these two competing factors based on numerical experiments. This gives a steep decay while allowing a more manageable time step.

Using the values of  $K_1$  and  $K_2$  and transforming equation (9) into Cartesian coordinates gives the following expressions for the repulsive force on a particle  $i$  from particle  $j$  in the x, y, and z directions as

$$f_{rep,ij,x} = \frac{Q}{8a^4} \left( e^{-12 \left[ \frac{r_{ij}}{2a} - 1 \right]} \right) \frac{x_{ij}}{r_{ij}} \quad (13)$$

$$f_{rep,ij,y} = \frac{Q}{8a^4} \left( e^{-12 \left[ \frac{r_{ij}}{2a} - 1 \right]} \right) \frac{y_{ij}}{r_{ij}} \quad (14)$$

$$f_{rep,ij,z} = \frac{Q}{8a^4} \left( e^{-12 \left[ \frac{r_{ij}}{2a} - 1 \right]} \right) \frac{z_{ij}}{r_{ij}} \quad (15)$$

For the physical interaction with the walls of the container, a similar approach was taken, and the equation developed for the interaction of a particle with the floor/ceiling is given as

$$f_{wiz} = \frac{Q}{8a^4} \left[ e^{-30 \left( \frac{z_i}{2a} - .5 \right)} - e^{-30 \left[ \frac{(H-z_i)}{2a} \right]} \right] \quad (16)$$

where  $f_{wiz}$  is the force on particle  $i$  from the wall in the z direction,  $z_i$  is the absolute distance from the bottom boundary to particle  $i$  in the z direction, and  $H$  is the total height of the volume (not to be confused with the use of  $H$  elsewhere as the magnetic field strength). Equations identical to (16) are used for the horizontal boundaries with the substitutions for the particles x and y positions (instead of  $z_i$ ) and the length and width of the containment area (instead of  $H$ ).

## **E. INTERACTION WITH ELECTROMAGNET**

Up to this point the discussion of the physics of the interactions of the particles in a MR fluid is exactly the same as if it was an ER fluid (replace the electromagnet with

charged parallel plate conductors and replace some of the magnetic constants with their electrical equivalents). A primary difference between the two arises in the physics of the interaction between the electromagnet (MR) and the interaction with the charged conducting plate (ER). In the latter case, the charged plates induce an electric dipole (exactly analogous to the electromagnets inducing a magnetic dipole), but the electric dipoles interact with the plates in an easily understood manner. The presence of the electric dipoles themselves will induce a current distribution on the plates and then these dipoles are electrically attracted to the plates because of this current distribution. A well documented manner to calculate this interaction is by the method of image charge [5]. Basically the interaction of a dipole that is a distance  $L$  from the plate is identical to assuming there is an infinite number of equal dipoles on the other side of the plate at distances  $nL$  where  $n=1,2,3,\dots$ . Therefore an electric dipole will interact with the conducting plate, specifically will be attracted to the plate and attach itself to the plate. If there are multiple dipoles, they will form chains, and the chains will anchor themselves to the plate and behave as if the chain was infinitely long. This is what allows an ER to have a shear stress; the chains are anchored to the plate.

There is no analogy in the MR case. There is no such thing as a magnetic current produced at the boundary of the electromagnet that would allow the use of the dipole image method to determine the interaction of the chain with the magnet [6]. Another way to look at this is to consider a single magnetic dipole between the magnets. Assuming a constant magnetic field, the dipole would not be attracted to either of the magnets. There seems to be nothing to lock the chain in place and therefore an MR fluid would not be able to have a shear stress. Experimentally, this is not true. The chains do become locked.

There are two reasonable theories as to how this locking occurs. The first is to question the assumption that the field is uniform. Away from the edges of the magnets, due to the small gap between the magnets, it is safe to assume a uniform field. When the magnets are close together the field lines away from the edges do not spread out and consequently there is no gradient. However, at the edges of the magnets, this is not true. The fields bulge outward and tend to wrap around, causing large gradients. One proposal



is that away from the edges of the magnets, the chains are free to move (are not locked to the magnet), but as the bulk fluid flow sweeps them toward the edge of the magnet, they become locked in this area of high field gradients and effectively form a lattice type wall. Other chains being swept along will then build up behind this lattice wall.

Another theory approach is to again to question the uniformity of the field, this time at the fluid/magnet interface. To explain this effect requires the use of Maxwell's laws. The equation of specific use is

$$\nabla \cdot \mathbf{B} = 0 \quad (17)$$

where  $B$  is magnetic flux density (Tesla). The relationship between  $H$  and  $B$  is given by

$$\mathbf{B} = \mu \mathbf{H} \quad (18)$$

where  $\mu$  is the magnetic permeability of the substance through which  $H$  exists. Using equations (17) to solve for the normal component of  $B$  across the discontinuity between the magnet and the fluid (there are no tangential components) implies

$$n_1 \cdot (\mu_2 H_2 - \mu_1 H_1) = 0 \text{ or } \mu_2 H_2 = \mu_1 H_1$$

where the subscripts refer to the magnetic permeability and magnetic field of the magnet and fluid respectively [8]. This shows at the interface between the magnet and fluid there is a jump discontinuity in the magnetic field (assuming that the magnetic permeability of the two materials are not equal).

The model presented here assumes the second explanation for a physical interaction between the magnet and dipoles. The exact force caused by this gradient is unknown, but it is assumed that it is incredibly short ranged, and that causes a force of attraction such that, when multiplied by the frictional coefficient between the particle and magnet, leads to a frictional force that is substantially larger in magnitude as compared to the force that tends to sweep the particle along. This assumption is valid since the force tending to sweep the particle along with the flow is a function the flow velocity at the particle's location. Since the particle is small (~5 microns) and resides at the interface, the flow velocity is approximately zero (no slip condition). In other word, a particle that happens to touch the magnet becomes locked in place, but particles in the stream, away from the wall, do not experience this force.

## IV. MODEL FOR INTERACTION

### A. NEWTON'S SECOND LAW

The description of a particle's motion in a MR fluid can be determined using Newton's second law of motion. In formulating a model for the motion of an arbitrary particle  $i$  apply this law in the x direction as follows

$$\sum F_{ix} = m \frac{d^2 x_i}{dt^2} \quad (19)$$

where the left hand side of the equation is the sum of all of the forces on particle  $i$  in the x direction and  $m$  is the particle's mass (not dipole moment). The left hand side includes the dipole interaction force, drag force, and repulsive forces due to contact with other particles and the walls. Combining equations (7), (10), (13) and (16) gives the following second order differential equation to solve

$$m \frac{d^2 x_i}{dt^2} + D \frac{dx_i}{dt} = F_{ix} \quad (20)$$

where  $D = 6\pi\eta a$ , and  $F_{ix} = F_{Mix} + \sum_{i \neq j}^N f_{rep,ij,x} + f_{wix}$ .

Equation (20) can be solved numerically, in its current form, using a range of techniques (for instance a Runge-Kutta algorithm). To make the computations more simple, integrate equation (20) over a sufficiently small time step  $\tau$  such that the term on the right hand side can be assumed constant. This gives an equation for the change in the position of the particle in the x direction during this time step  $\tau$  as shown below

$$\Delta x = \frac{F_{ix}\tau}{D} + \frac{V_0 m}{D} \left[ 1 - e^{-\frac{D\tau}{m}} \right] \quad (21)$$

where  $V_0$  is the velocity of the particle in the x direction at the beginning of the time step. This equations shows that if  $\tau$  is chosen such that it is several orders of magnitude less than  $m/D$  then the second term on the right hand side can be ignored and therefore

$$\Delta x = \frac{F_{ix}\tau}{D} \quad (22)$$

and similarly

$$\Delta y = \frac{F_{iy}\tau}{D} \quad (23)$$

$$\Delta z = \frac{F_{iz}\tau}{D} \quad (24)$$

for the y and z components. For the MR fluids analyzed here a typical value of  $m/D$  is about  $5\text{E-}7 \text{ sec}^{-1}$  which makes the time step on the order of  $1\text{E-}9 \text{ sec}$ . In reality this will be the upper limit on the time step. Initially a much smaller time step will be used in the computer simulation. This is due to how the program randomly establishes the initial positions of the particles and that they tend to overlap. A smaller time step is required to “push” the particles off of each other and the wall without destabilizing the computations with excessively large positional changes at each time step.

## B. STATIC FLUID MODEL

A computational algorithm was written to determine the dynamic motion of the particles in a MR fluid. The program takes user inputs for the length, width and height of the MR fluid area, the number of particles to simulate, the magnitude of the applied magnetic field (program assumes the direction is in the negative z direction), and the number of time steps to perform the algorithm. The program then randomly distributes the particles inside of the fluid area. Using this distribution the initial spacing between all of the particles is computed (the values of  $x_{ij}$ ,  $y_{ij}$ ,  $z_{ij}$  and  $r_{ij}$ ). Then the value of the dipole strength and drag coefficient is computed. Using the spacing between particles and the

value of the dipole moments,  $F_{ix}$ ,  $F_{iy}$ , and  $F_{iz}$  are calculated for every particle. If the particle is near the upper or lower wall (a distance between  $a$  and  $1.3a$ ) the forces are assumed zero for the reason of the interaction with the magnet/fluid boundary discussed in Chapter III. Then the forces are computed using equations (20). A time step is computed based on the value of  $m/D$  as described in the previous section. The updated position of every particle is then calculated using equations (22-24) and this new position is stored and plotted graphically if desired. This process is repeated for every time step using the updated positions from the previous time step.

As discussed above, a minor issue arises in the initial random spacing, especially at higher particle densities. Sometimes the particles are randomly placed such that two or more particles are spaced where the distance between them is less than their diameter length apart or such that the spacing between a particle and a wall is less than the particles radius length apart. This is not physically possible since the particles and the wall are hard. To overcome this, the time step chosen for the first 10 time steps is several orders of magnitude less than what is used for the remainder of the computation. This allows the repulsive force terms to “push” the particles away from each other and the wall without creating an abnormally large positional change that would eject them from the MR fluid domain. A copy of the computer code used is attached in Appendix B with a more detailed discussion as to the inner workings.

## C. DYNAMIC FLUID MODEL

The programs constructed to compute the dynamic motion of particles in a dynamic fluid are very similar to the one for the static case with a few alterations. Two separate programs were created, one for pressure driven flow and the other for shear driven flow (these were the only two specific flow types analyzed).

In the pressure driven case (parallel flow with a parabolic velocity distribution) it is assumed that the flow velocity is in the x direction, does not vary in the x and y directions and varies with a parabolic distribution in the z direction. The user inputs the meanline (maximum) flow and the program computes the value of the velocity at every

point in the MR fluid. Using this velocity distribution, another term is added to the right hand side of equation (20) to account for the drag force due to the fluid flow. Equation (20) now becomes

$$m \frac{d^2 x_i}{dt^2} + D \frac{dx_i}{dt} = F_{ix} + D U_i \quad (25)$$

where  $U_i$  is the flow velocity at the position of particle  $i$ . Note that since the flow is only in the x direction no modification is required for the equations of motion in the y and z directions. Applying the same arguments above that allowed for the inertial term to be ignored allows for the computation of the change in the position of the particle in the same manner as for the static case.

The program for the shear driven flow (Couette flow) is the same as for the pressure driven flow, but here the user specifies the flow velocity at the upper plate. The program then calculates the velocity at all other points in the fluid and simulates the particle motion exactly the same as for the pressure driven flow.

## V. SIMULATION RESULTS

### A. STATIC FLUID SIMULATION

The first qualitative analysis to examine is the effect on time response of the fluid as a function of particle density. The results shown are for three simulations where all parameters are held constant with the exception of particle density. The various parameters used are shown in the below table. In all cases the size of the rectangular volume is 100 X 100 X 100 micrometers with hard walls bounding the area. The magnetic field is applied in the negative z direction. The value of  $m/D$  used to calculate the time step has a value of 1.744E-7 based on the below parameters.

	Number of Particles	Fluid Viscosity	Fluid Permeability	Particle Permeability	Applied Magnetic Field
Simulation 1	40	.25 Pa s	1.26E-6 N/A <sup>2</sup>	.00377 N/A <sup>2</sup>	200 kA/m
Simulation 2	70	.25 Pa s	1.26E-6 N/A <sup>2</sup>	.00377 N/A <sup>2</sup>	200 kA/m
Simulation 3	100	.25 Pa s	1.26E-6 N/A <sup>2</sup>	.00377 N/A <sup>2</sup>	200 kA/m

Table 1. Parameters for Simulations 1, 2 and 3

The simulations were conducted out for 100,000 time steps which equates to a simulation time of 1.7 milliseconds. The figures below show the particle microstructures at various times for the above simulations in both a 3-D and top down view.

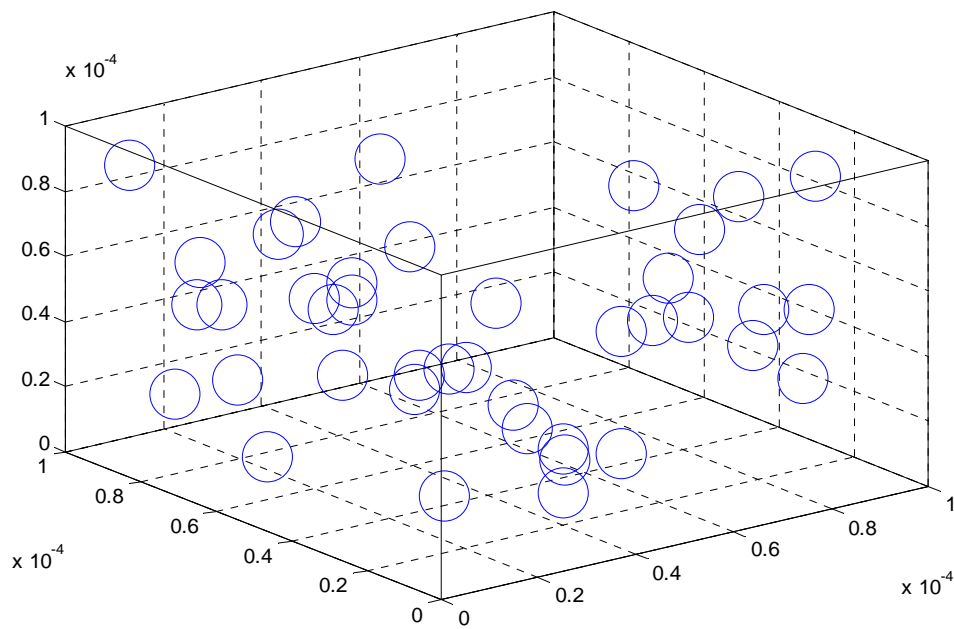


Figure 4. Simulation 1, Initial Particle Distribution, 3-D View

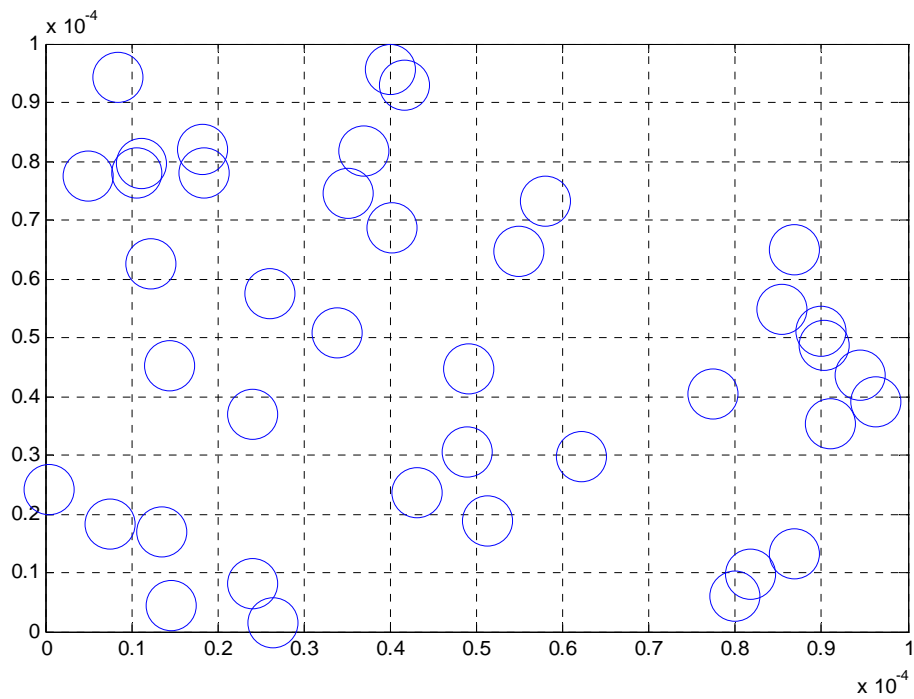


Figure 5. Simulation 1, Initial Particle Distribution, Top Down View

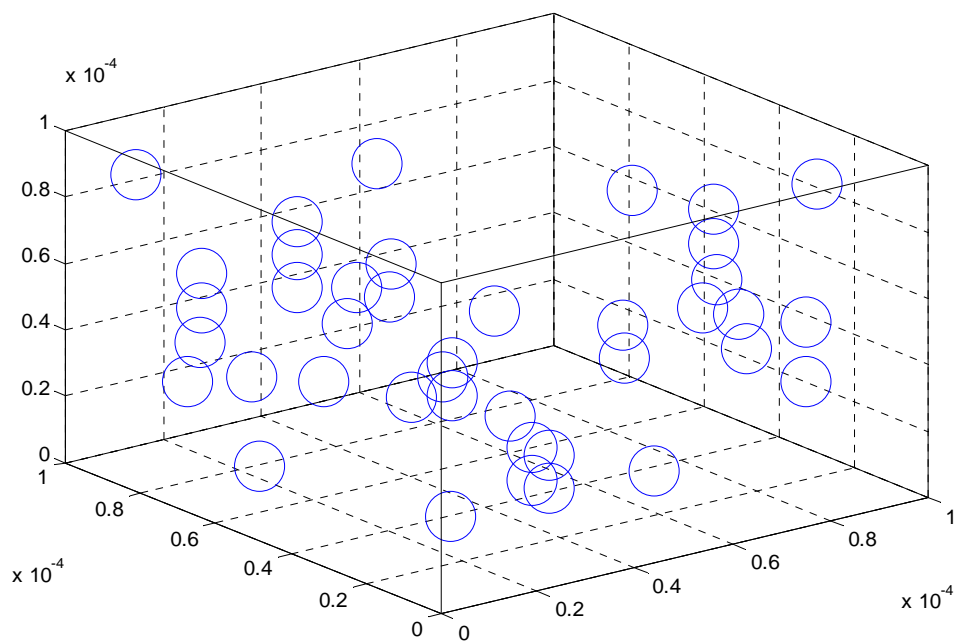


Figure 6. Simulation 1, Time = 0.16 milliseconds, 3-D View

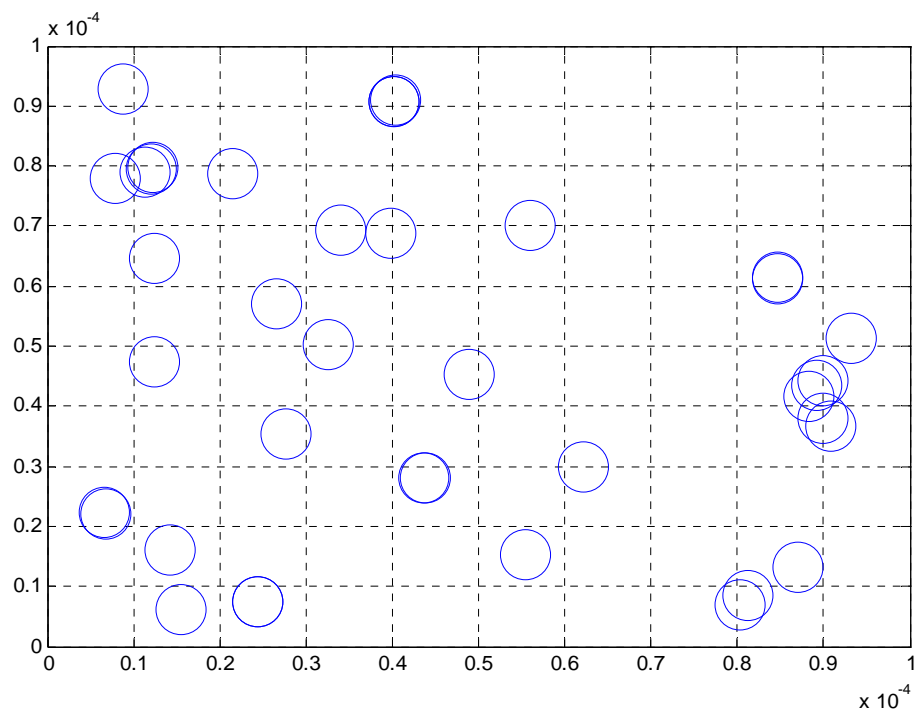


Figure 7. Simulation 1, Time = 0.16 milliseconds, Top Down View



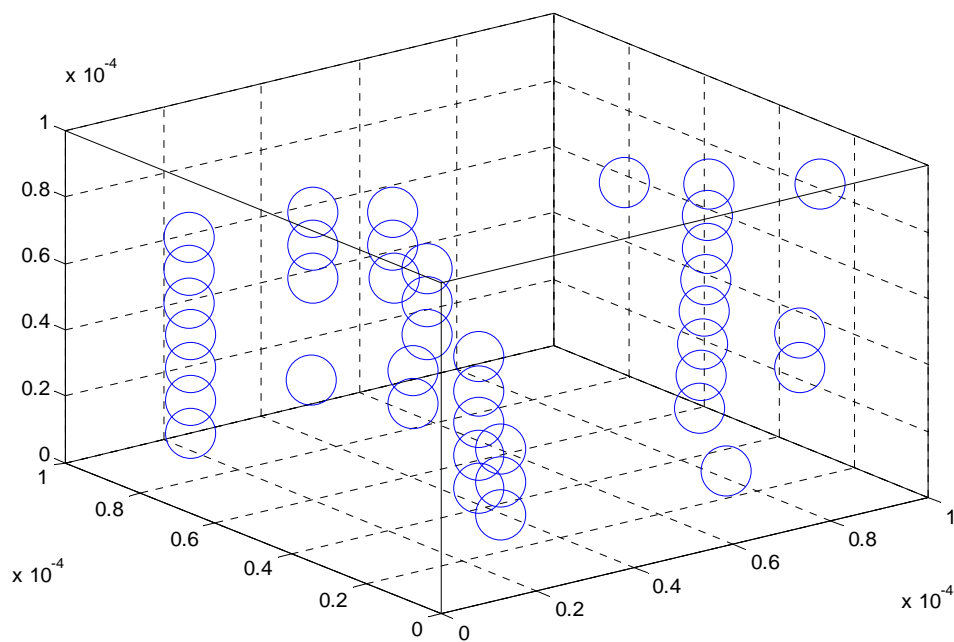


Figure 8. Simulation 1, Time = 1.7 milliseconds, 3-D View

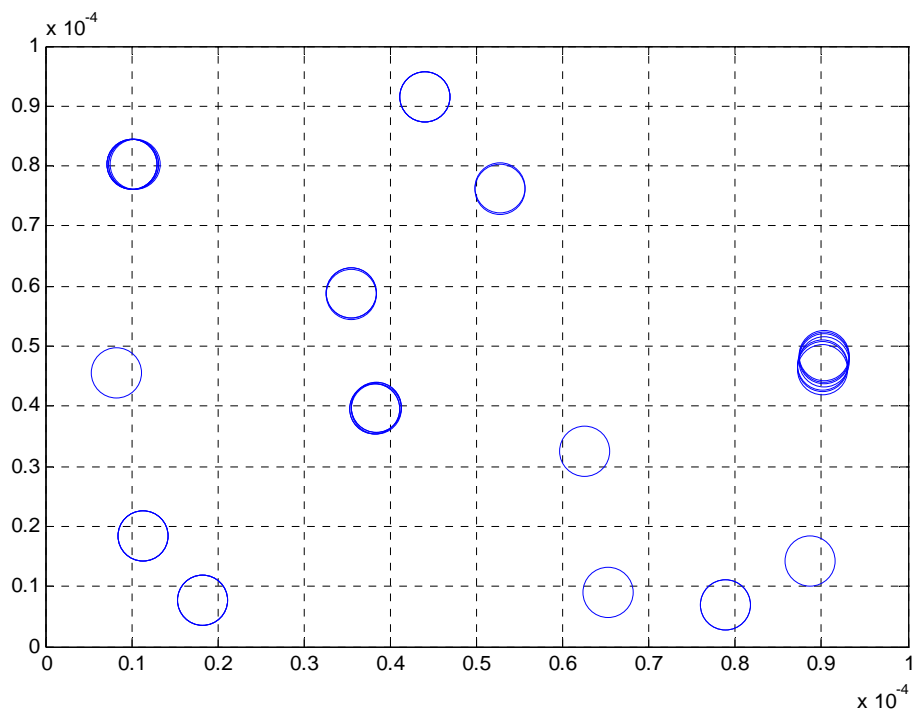


Figure 9. Simulation 1, Time = 1.7 milliseconds, Top Down View

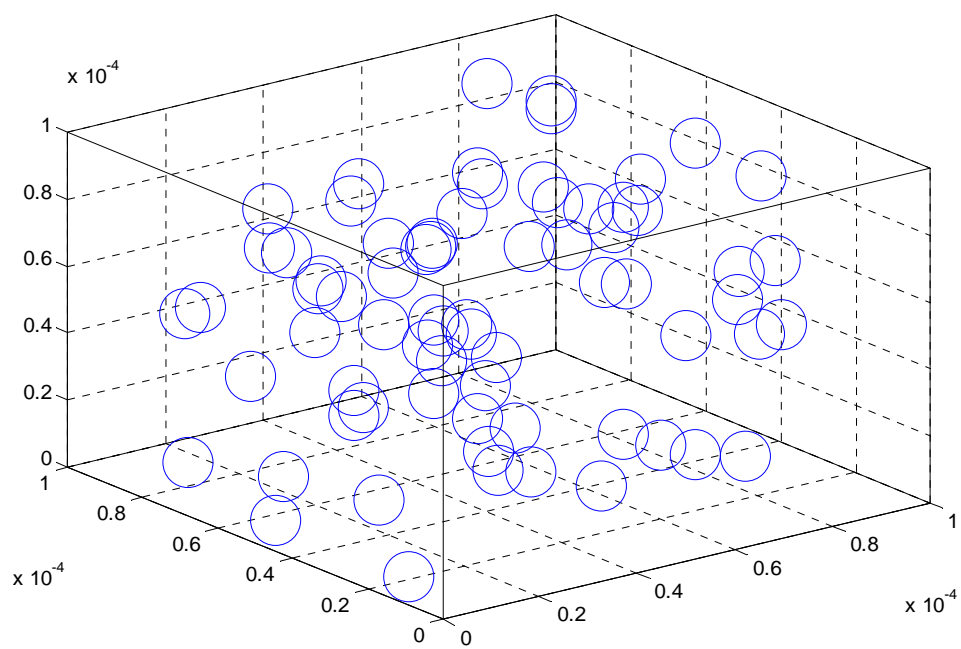


Figure 10. Simulation 2, Initial Particle Distribution, 3-D View

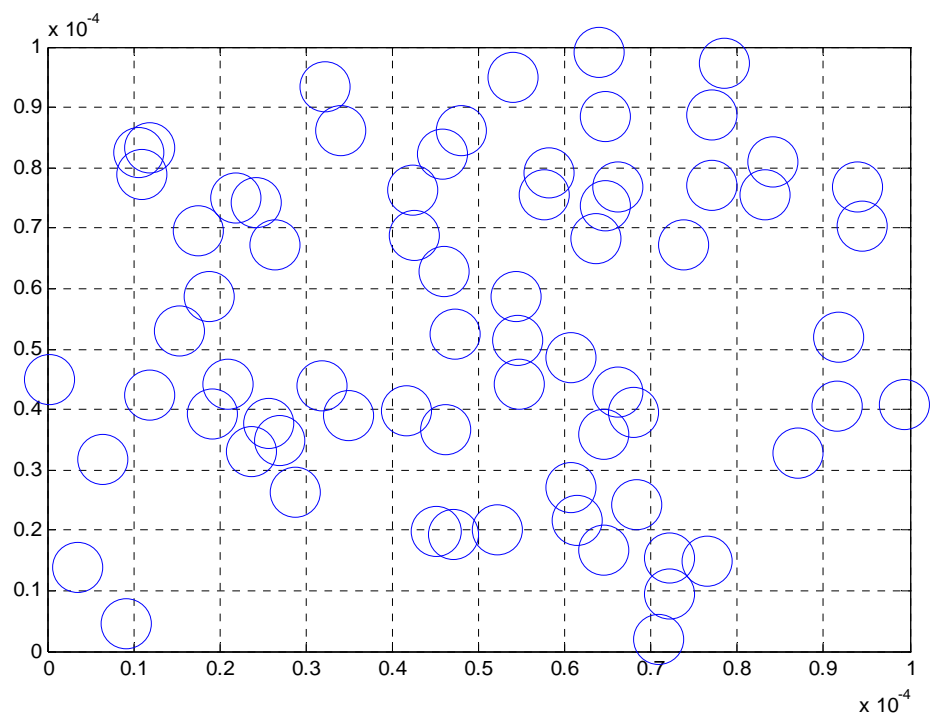


Figure 11. Simulation 2, Initial Particle Distribution, Top Down View

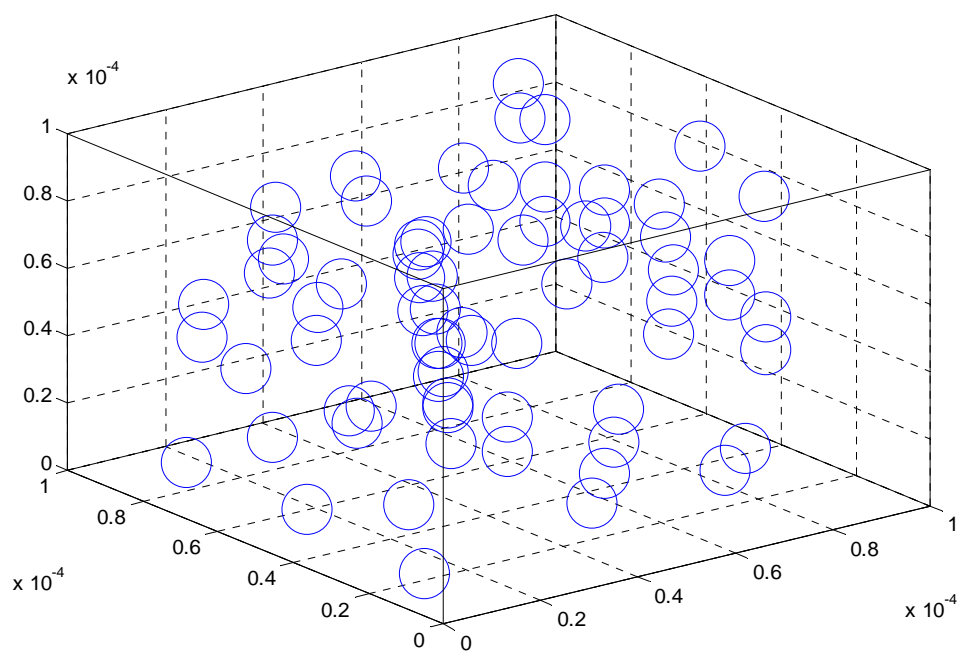


Figure 12. Simulation 2, Time = 0.16 milliseconds, 3-D View

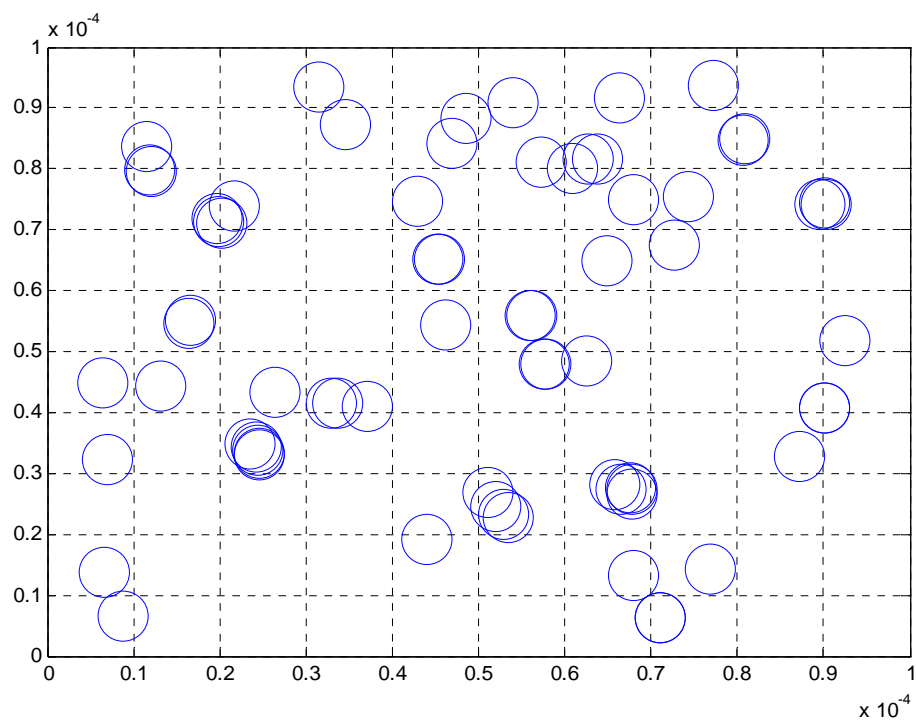


Figure 13. Simulation 2, Time = 0.16 milliseconds, Top Down View

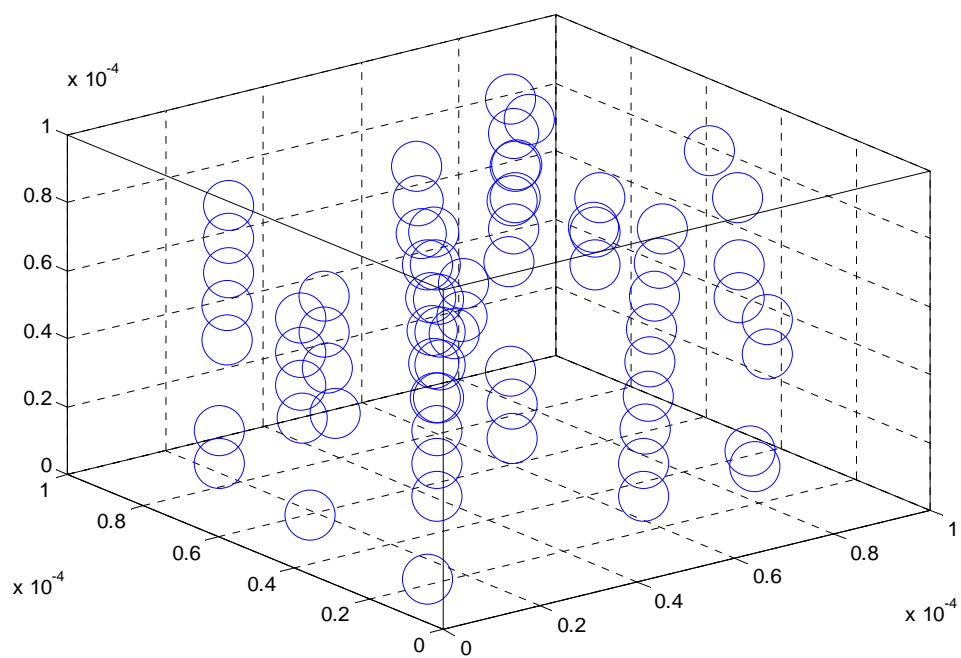


Figure 14. Simulation 2, Time = 0.86 milliseconds, 3-D View

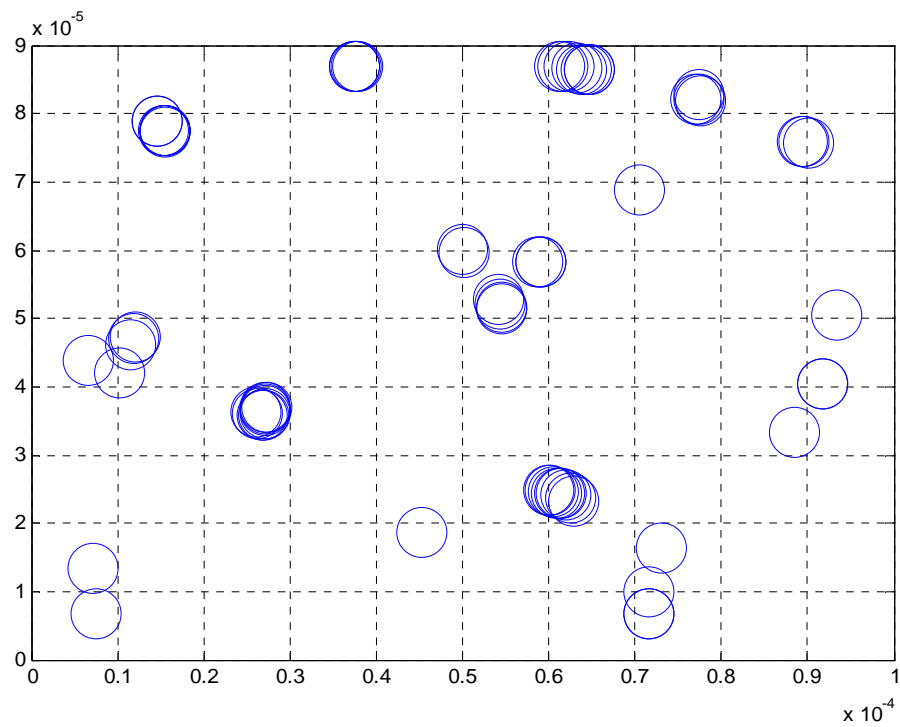


Figure 15. Simulation 2, Time = 0.86 milliseconds, Top Down View

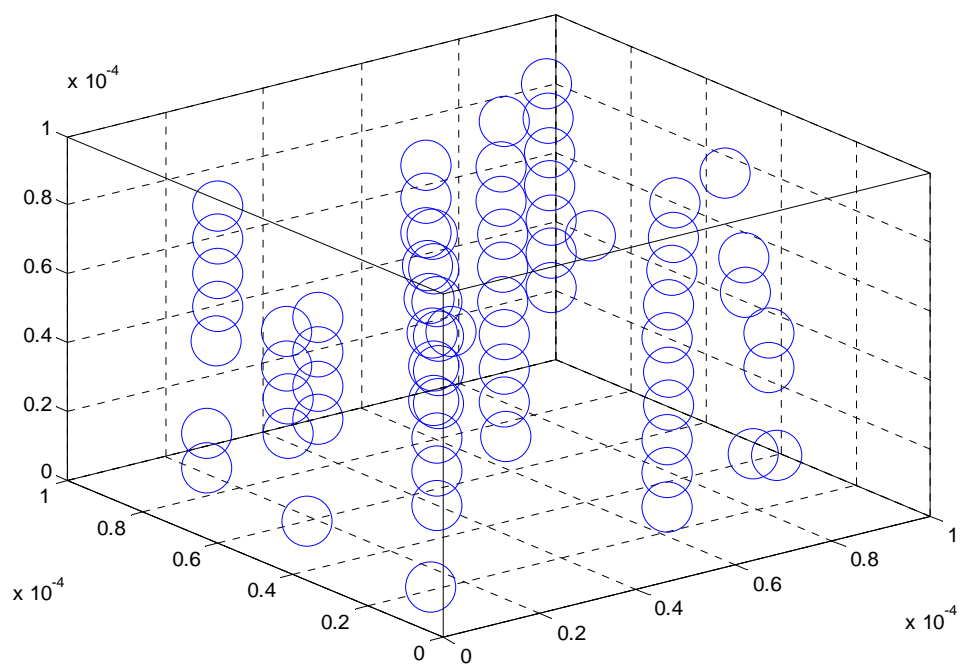


Figure 16. Simulation 2, Time = 1.7 milliseconds, 3-D View

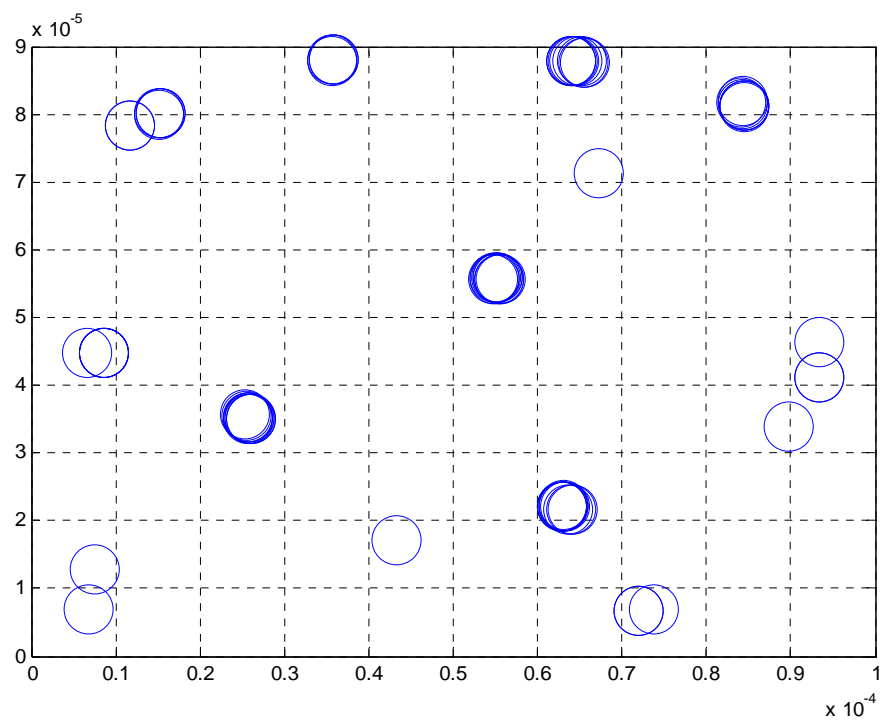


Figure 17. Simulation 2, Time = 1.7 milliseconds, Top Down View

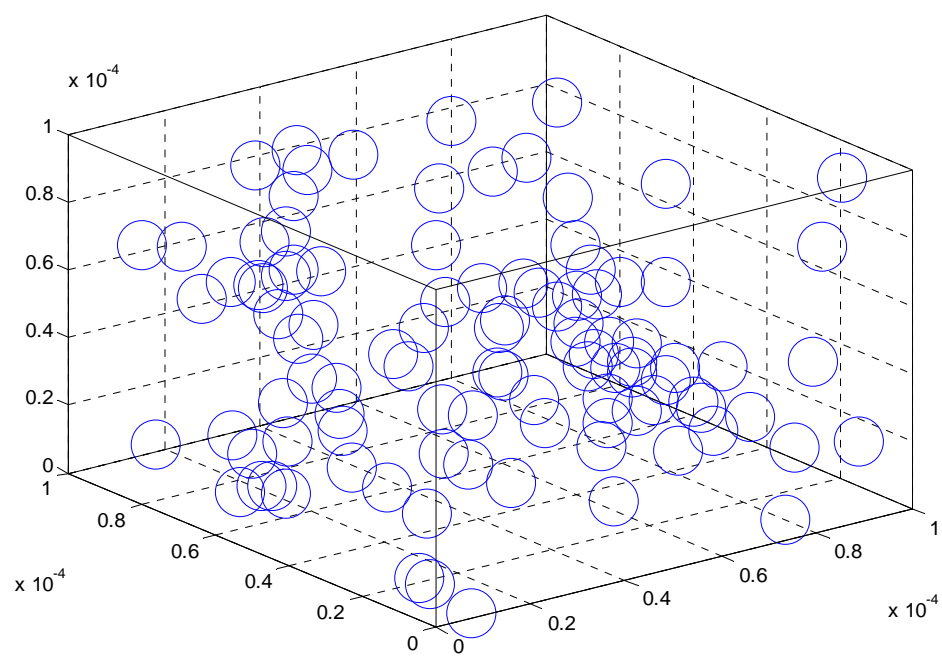


Figure 18. Simulation 3, Initial Particle Distribution, 3-D View

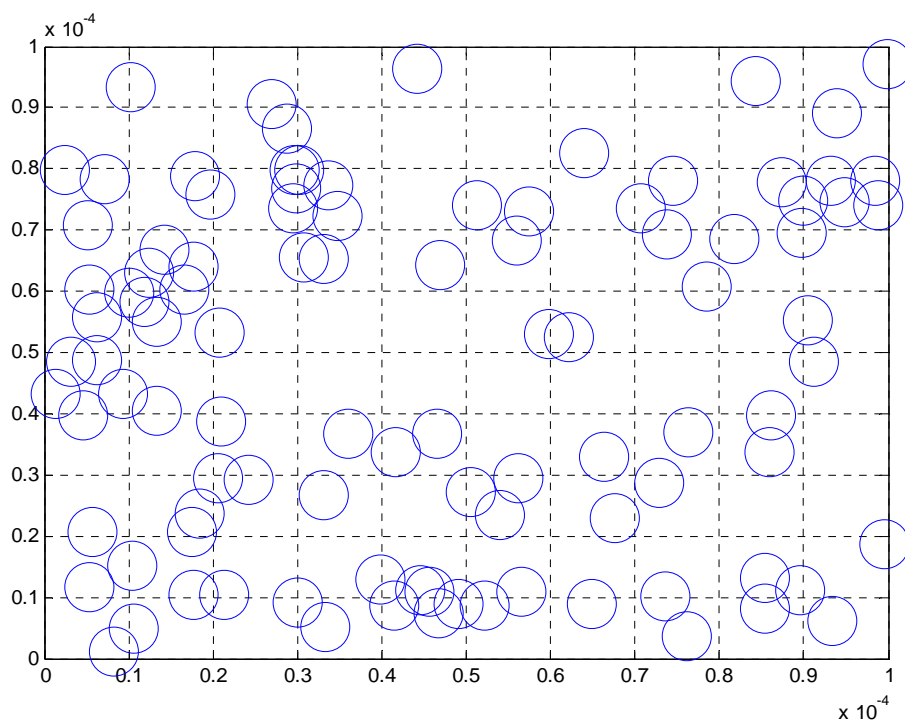


Figure 19. Simulation 3, Initial Particle Distribution, Top Down View

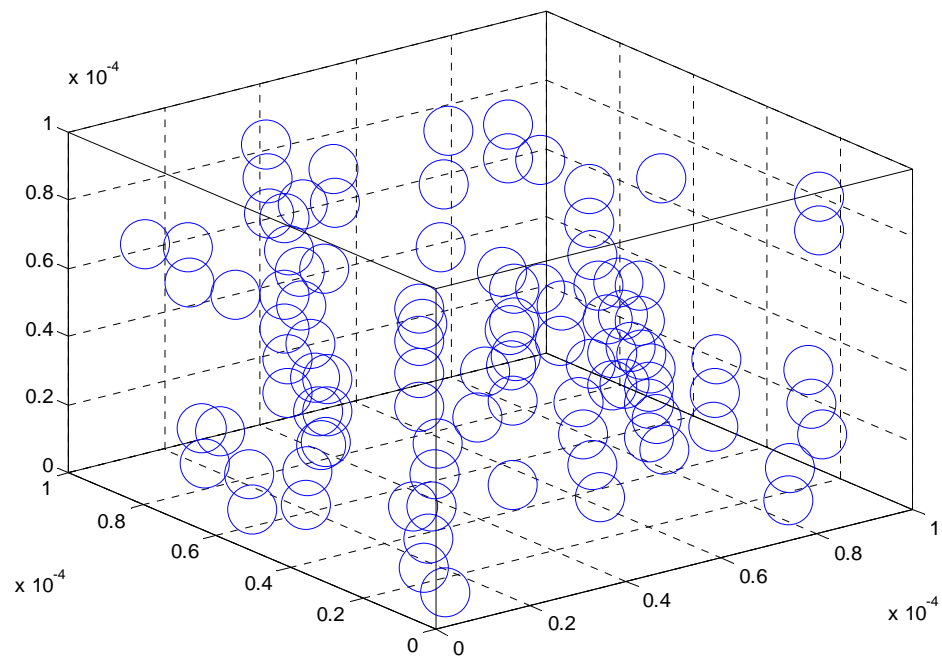


Figure 20. Simulation 3, Time = 0.16 milliseconds, 3-D View

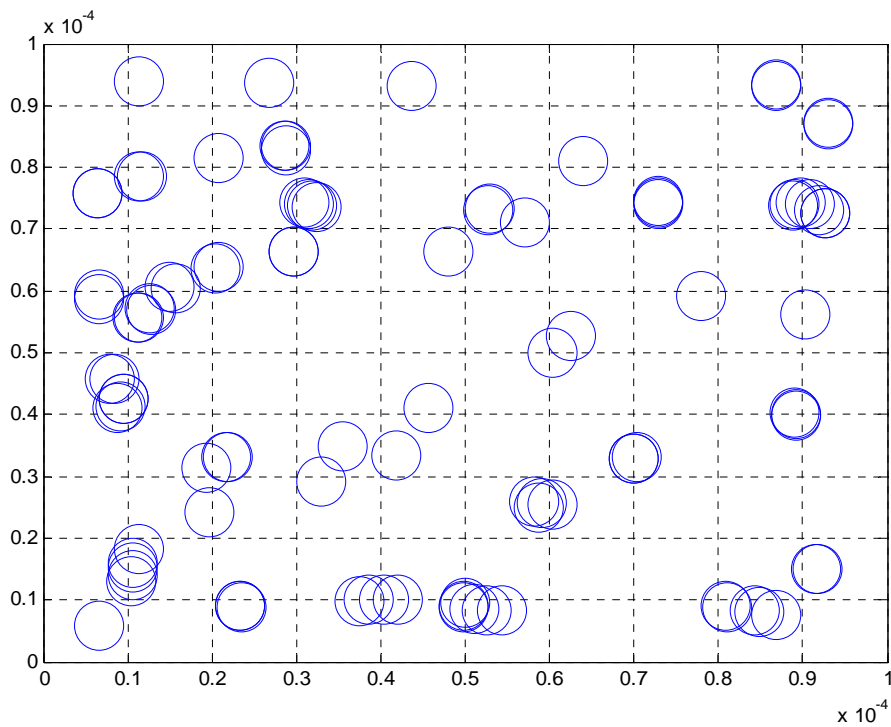


Figure 21. Simulation 3, Time = 0.16 milliseconds, Top Down View

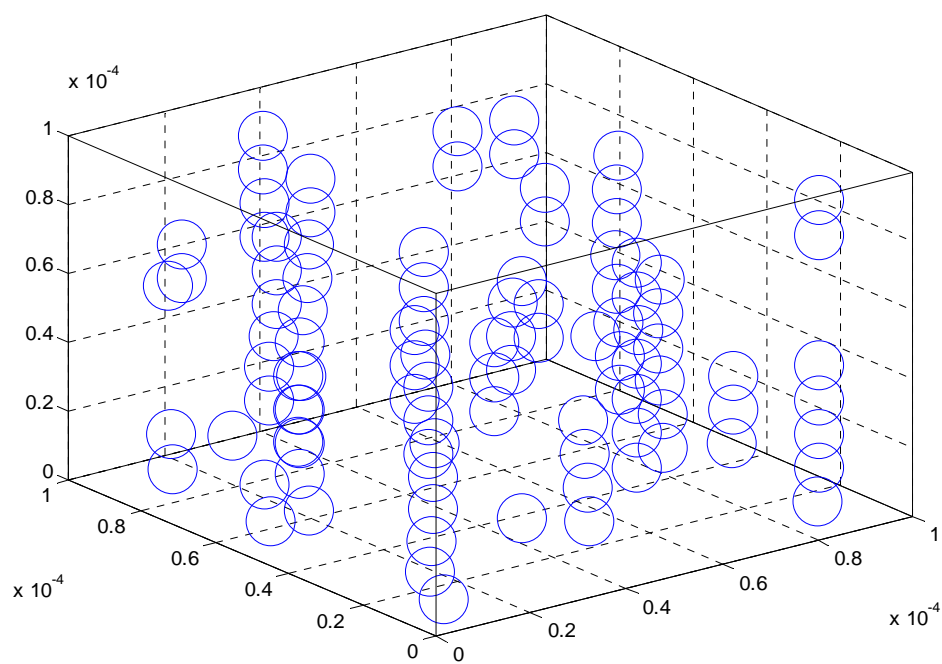


Figure 22. Simulation 3, Time = 0.86 milliseconds, 3-D View

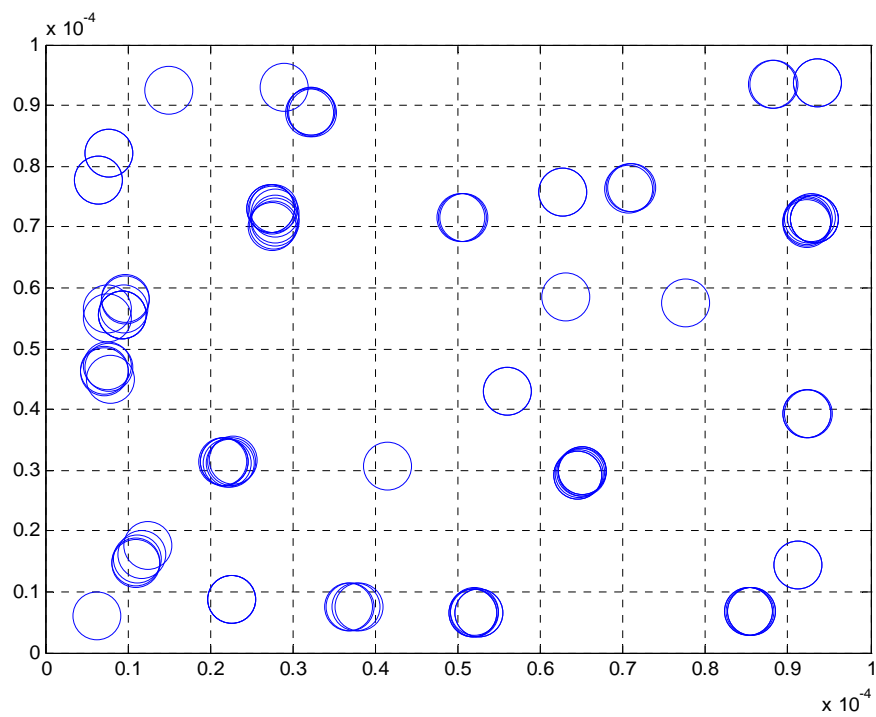


Figure 23. Simulation 3, Time = 0.86 milliseconds, Top Down View



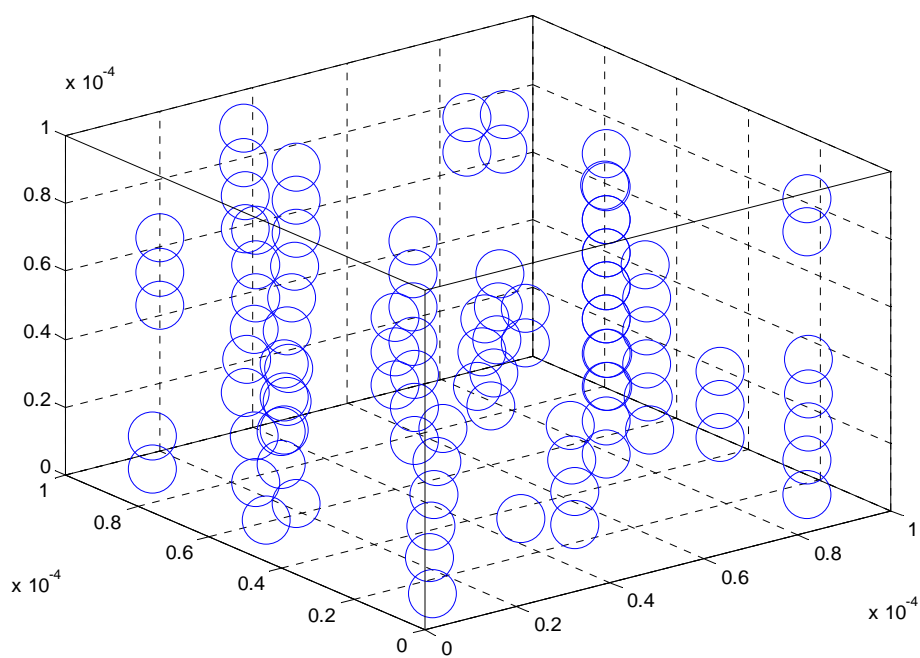


Figure 24. Simulation 3, Time = 1.7 milliseconds, 3-D View

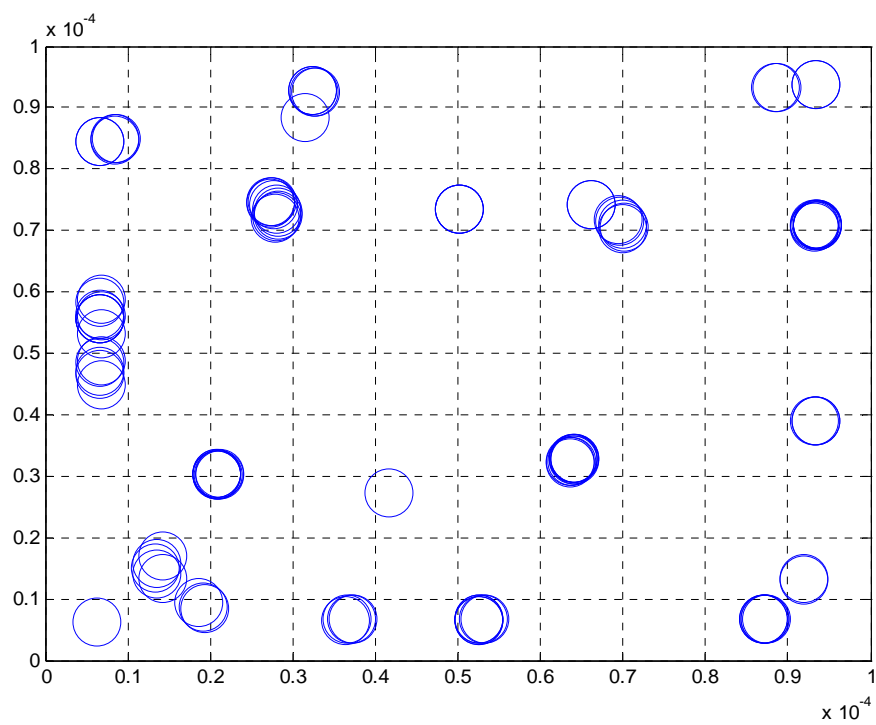


Figure 25. Simulation 3, Time = 1.7 milliseconds, Top Down View

Qualitatively, from the above figures, it is apparent that the speed at which the particles form chains is a function of the density of the particles in the fluid. Examining the two extreme cases (Simulations 1 and 3), much longer structures with fewer smaller structures are evident in Figure 20 than exist in Figure 6. Therefore, this model demonstrates the experimentally verified fact that particle density is a factor in response time of the MR fluid [3].

The second qualitative analysis to examine is the effect on time response of the fluid as a function of applied magnetic field strength. The results shown are for three simulations where all parameters are held constant with the exception of the magnetic field. The various parameters used are shown in Table 2. In all cases the size of the rectangular volume is 100 X 100 X 100 micrometers with hard walls bounding the area. The magnetic field is applied in the negative z direction. The value of  $m/D$  used to calculate the time step has a value of 1.744E-7 based on the below parameters.

	Number of Particles	Fluid Viscosity	Fluid Permeability	Particle Permeability	Applied Magnetic Field
Simulation 1	70	.25 Pa s	1.26E-6 N/A <sup>2</sup>	.00377 N/A <sup>2</sup>	150 kA/m
Simulation 2	70	.25 Pa s	1.26E-6 N/A <sup>2</sup>	.00377 N/A <sup>2</sup>	200 kA/m
Simulation 3	70	.25 Pa s	1.26E-6 N/A <sup>2</sup>	.00377 N/A <sup>2</sup>	250 kA/m

Table 2. Parameters for Simulations 4, 5 and 6

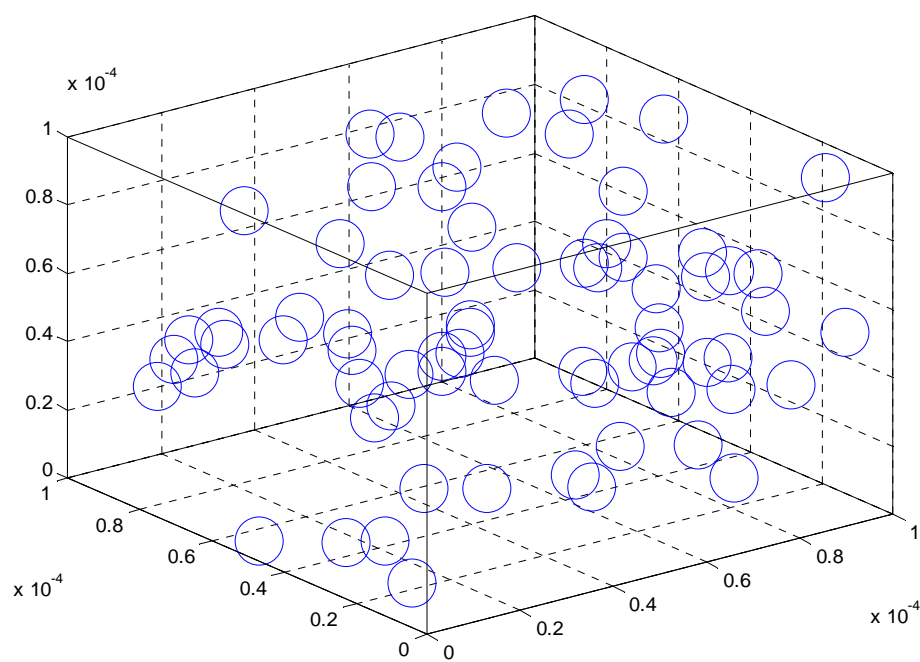


Figure 26. Simulation 4, Initial Particle Distribution, 3-D View

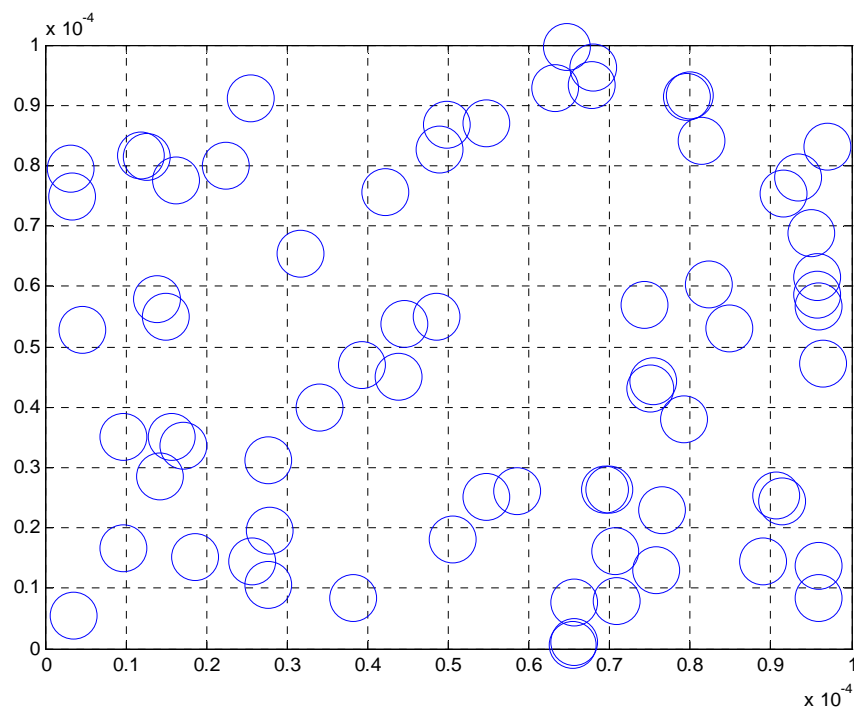


Figure 27. Simulation 4, Initial Particle Distribution, Top Down View

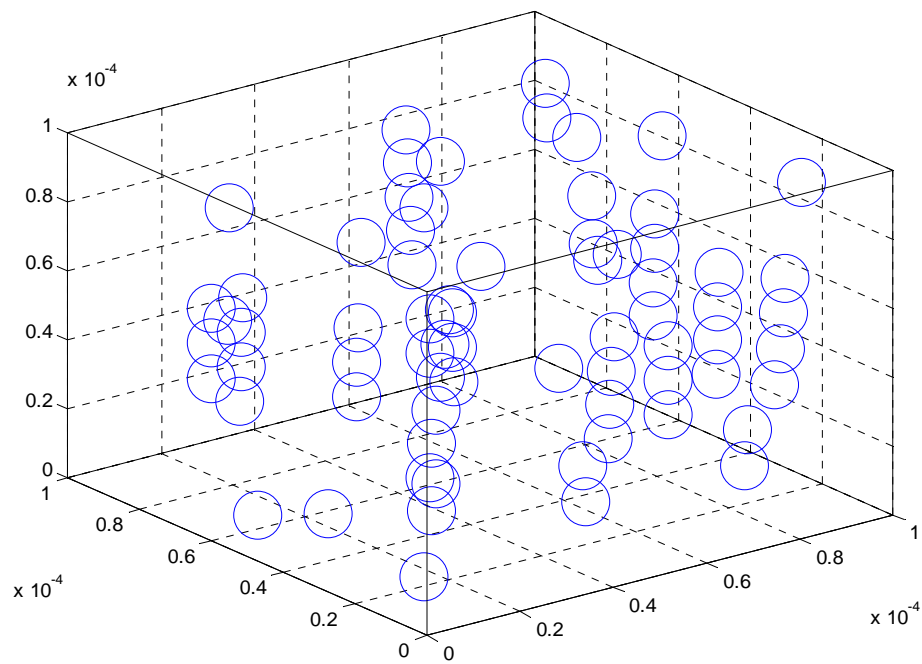


Figure 28. Simulation 4, Time = 0.86 milliseconds, 3-D View

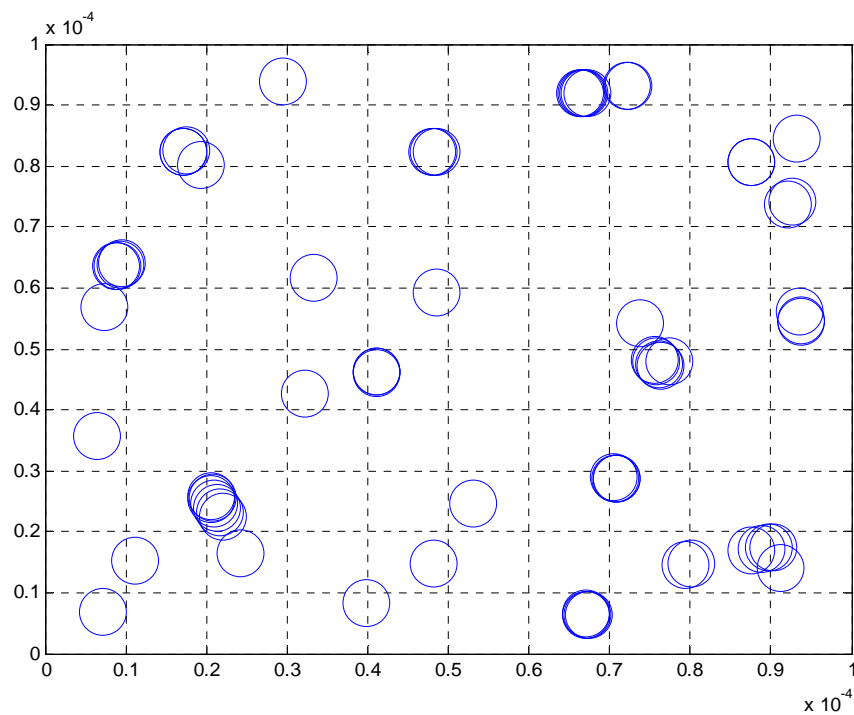


Figure 29. Simulation 4, Time = 0.86 milliseconds, Top Down View

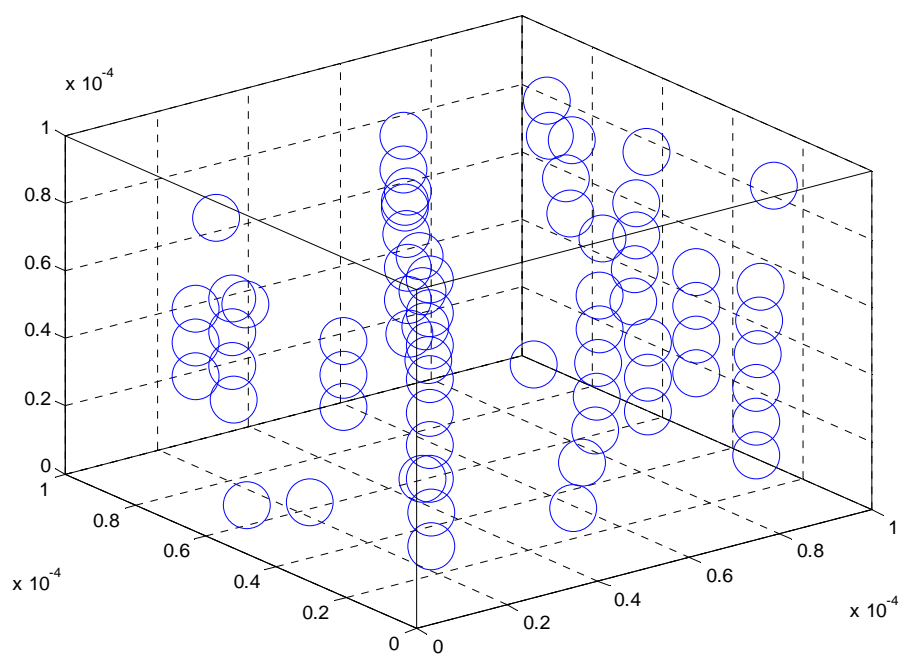


Figure 30. Simulation 4, Time = 1.7 milliseconds, 3-D View

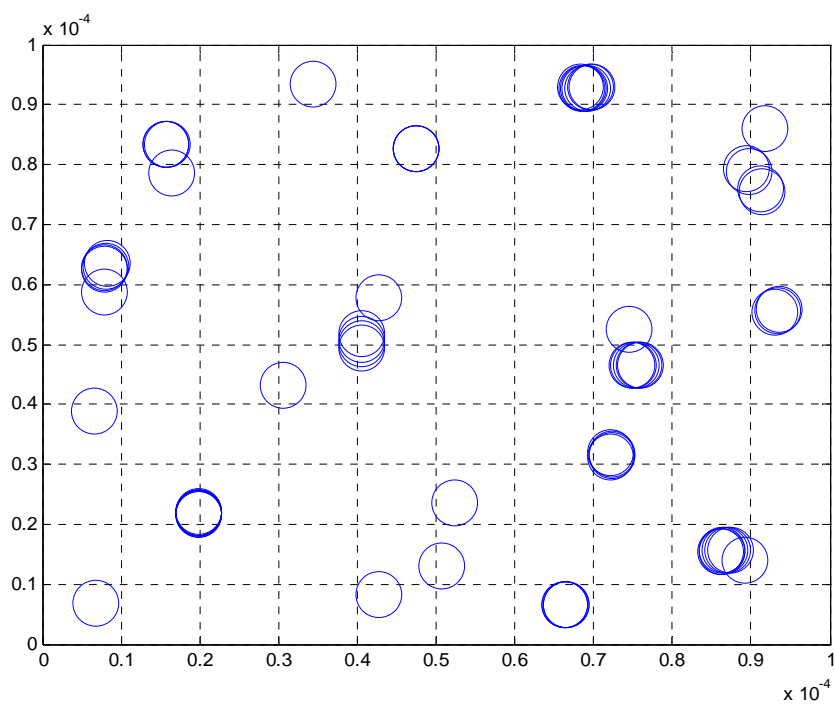


Figure 31. Simulation 4, Time = 1.7 milliseconds, Top Down View

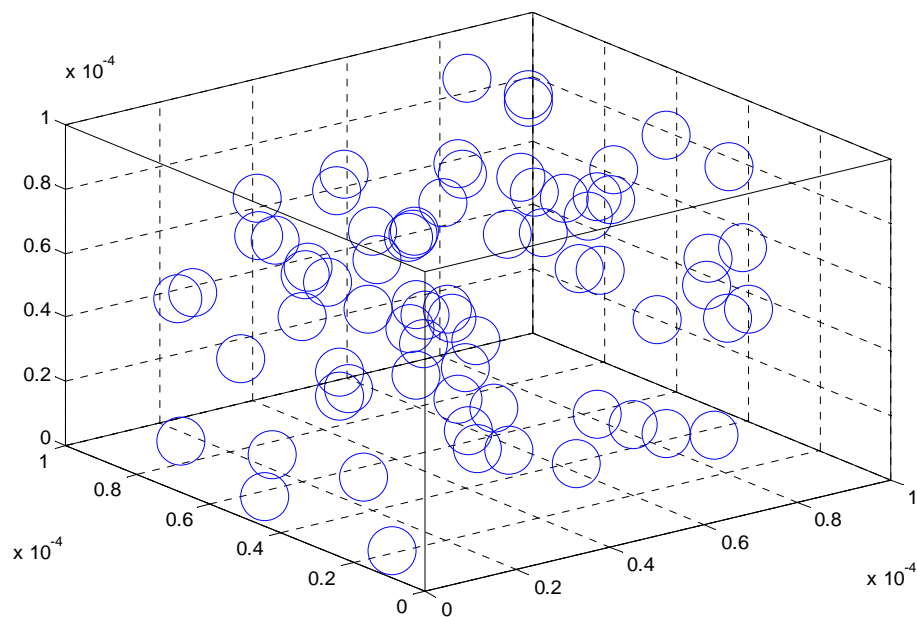


Figure 32. Simulation 5, Initial Particle Distribution, 3-D View

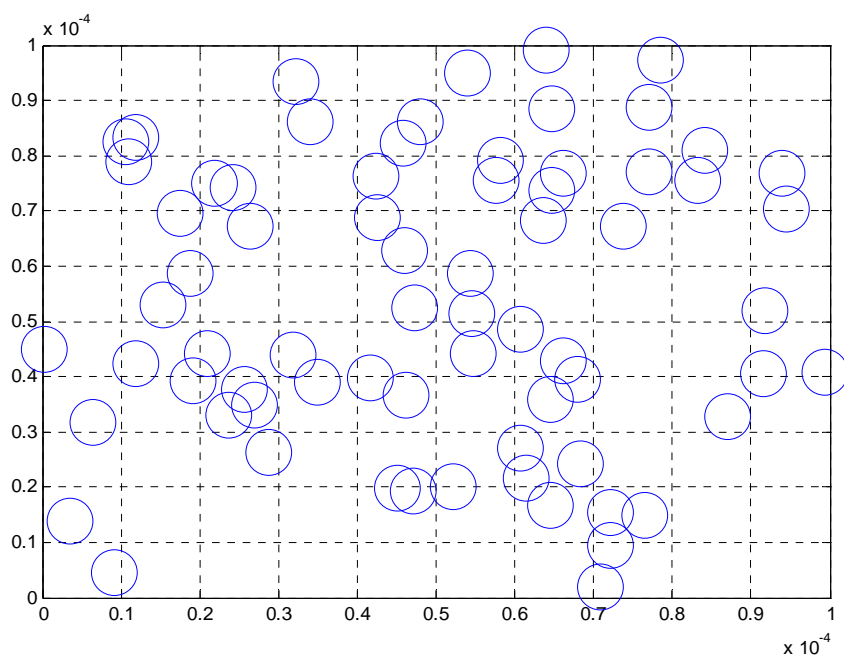


Figure 33. Simulation 5, Initial Particle Distribution, Top Down View

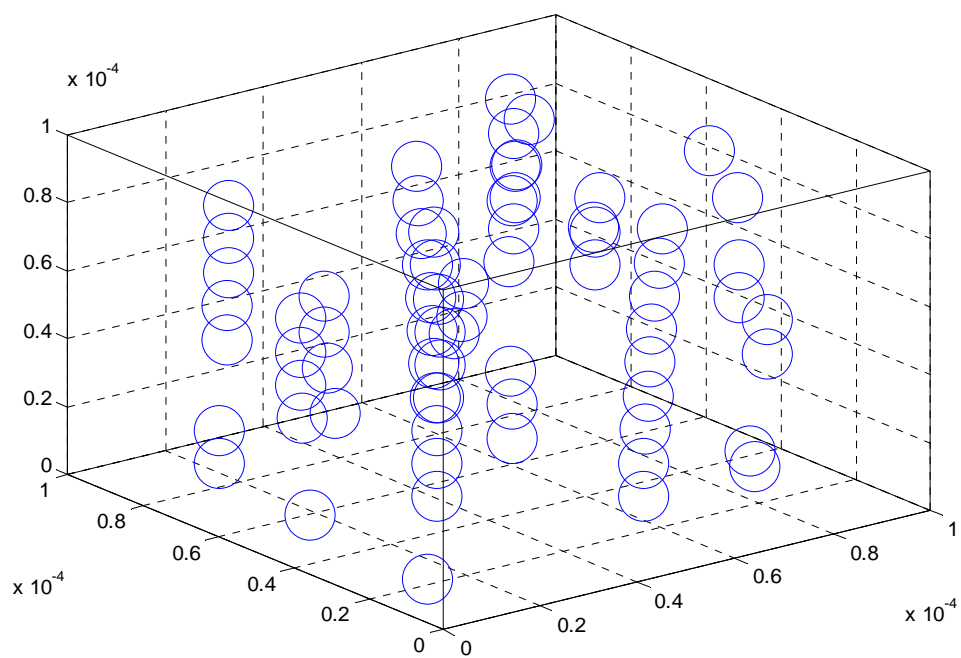


Figure 34. Simulation 5, Time = 0.86 milliseconds, 3-D View

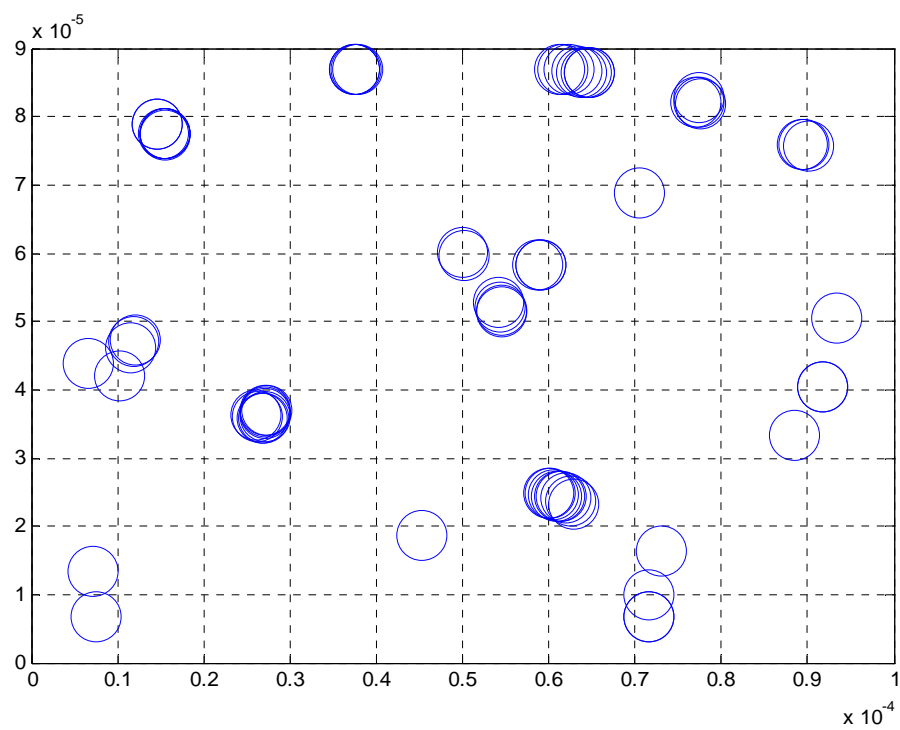


Figure 35. Simulation 5, Time = 0.86 milliseconds, Top Down View

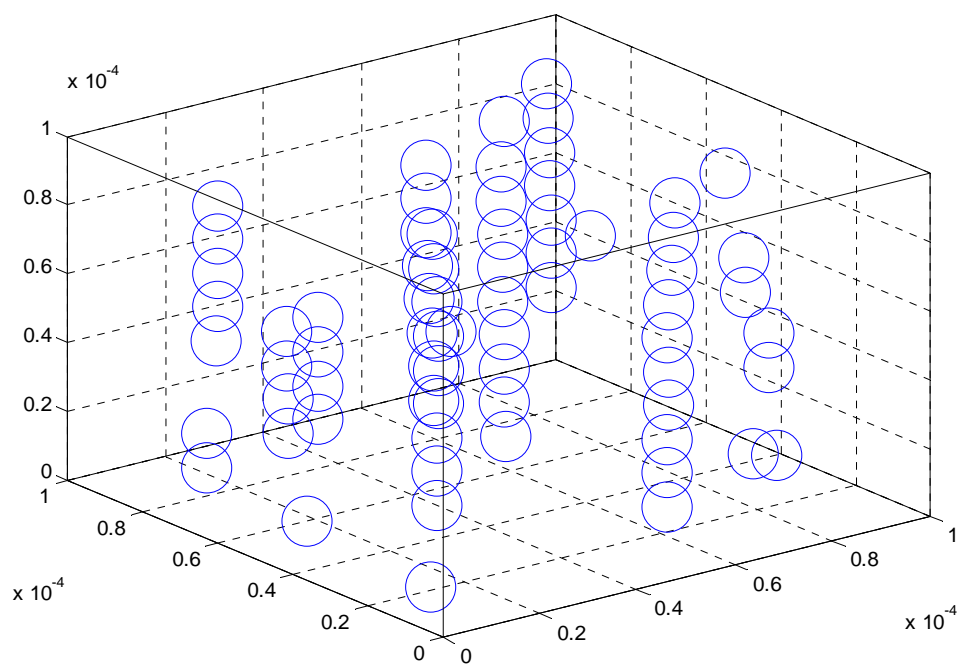


Figure 36. Simulation 5, Time = 1.7 milliseconds, 3-D View

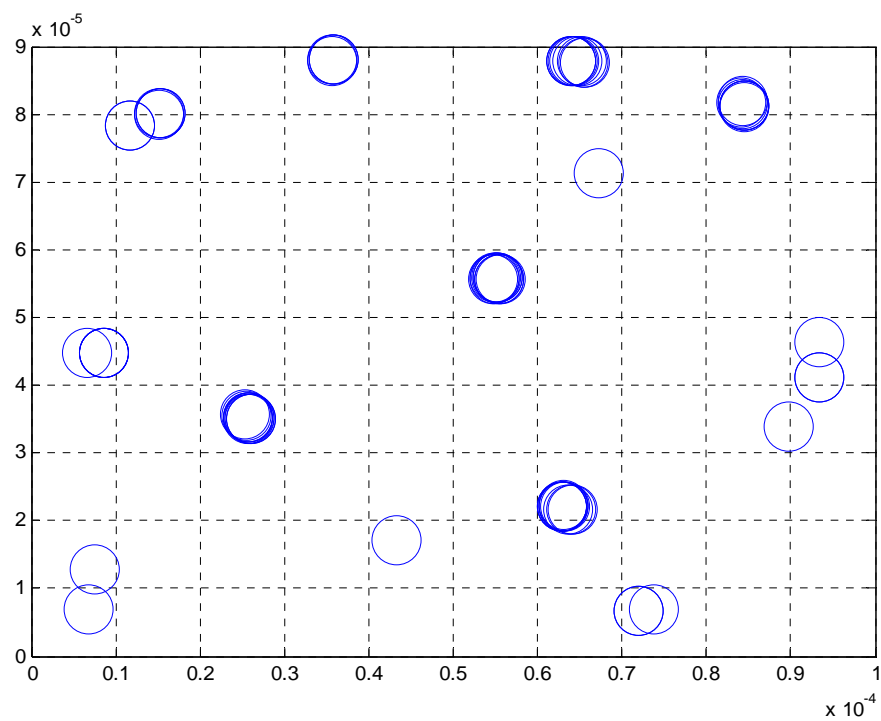


Figure 37. Simulation 5, Time = 1.7 milliseconds, 3-D View



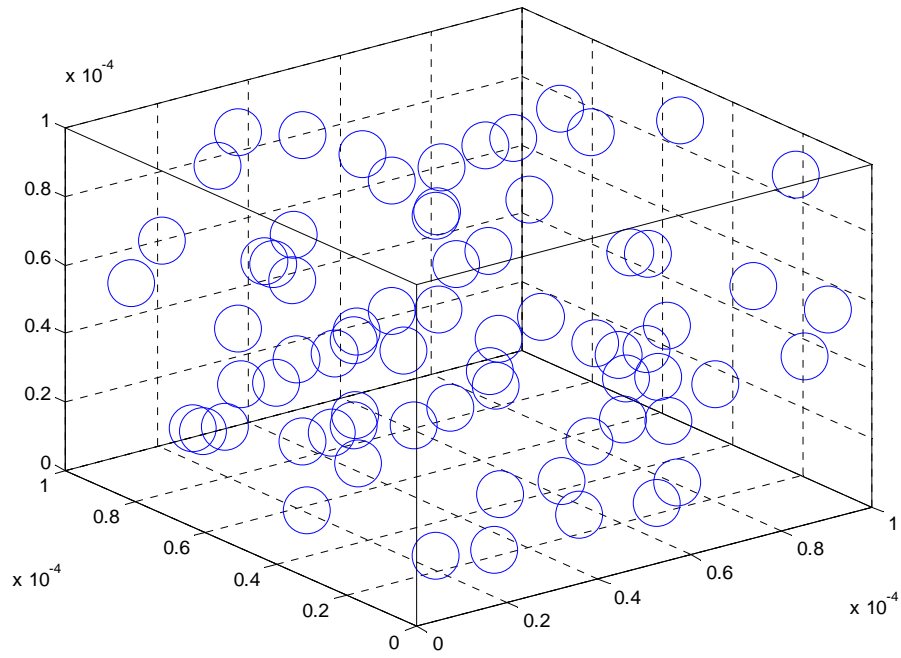


Figure 38. Simulation 6, Initial Particle Distribution, 3-D View

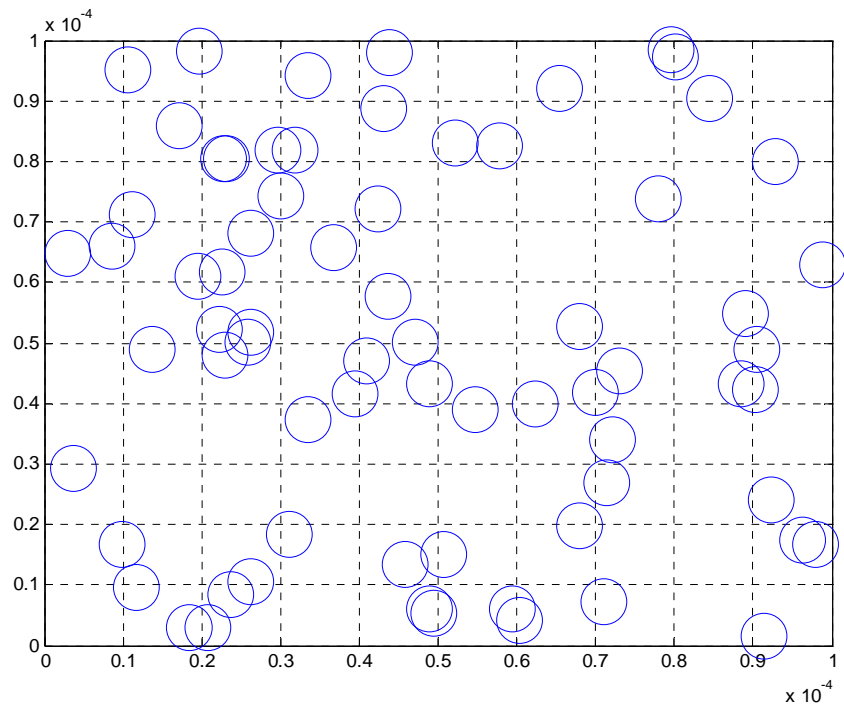


Figure 39. Simulation 6, Initial Particle Distribution, Top Down View

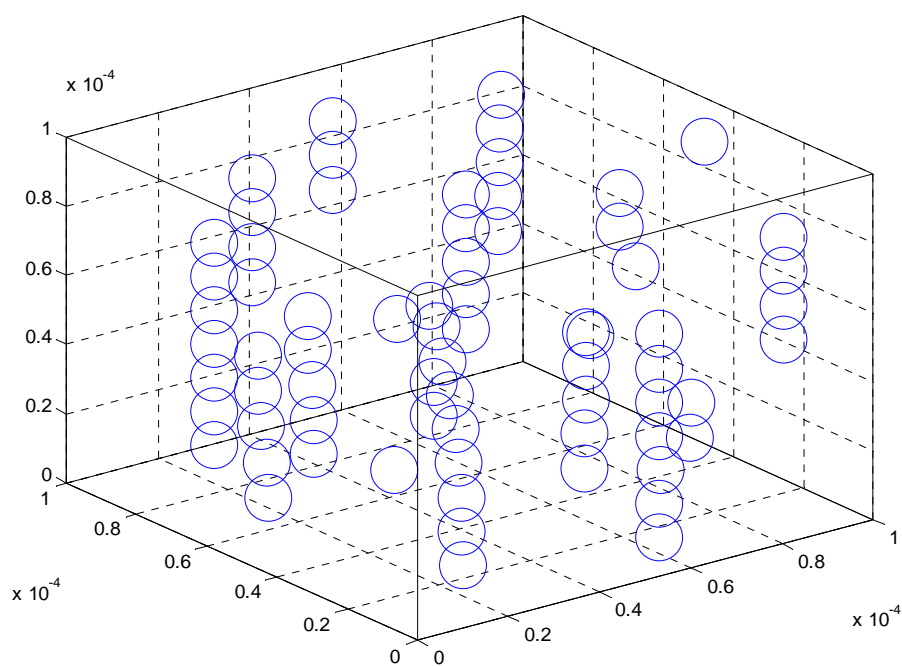


Figure 40. Simulation 6, Time = 0.86 milliseconds, 3-D View

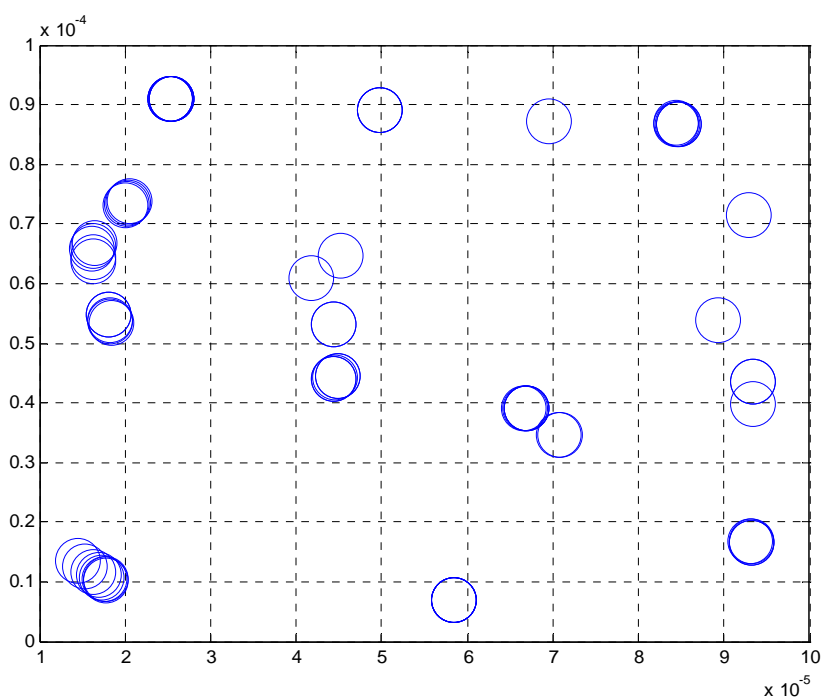


Figure 41. Simulation 6, Time = 0.86 milliseconds, Top Down View

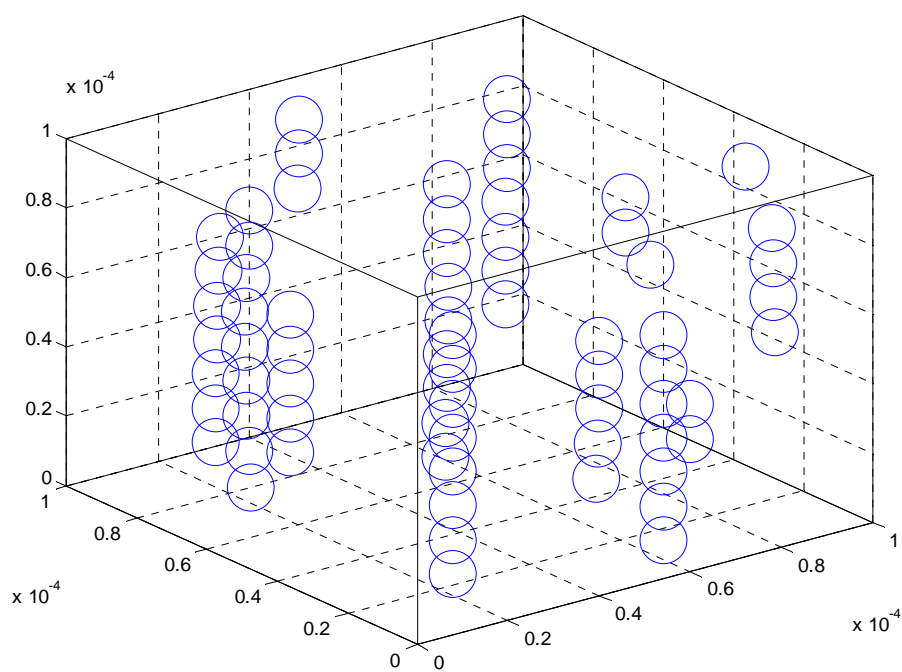


Figure 42. Simulation 6, Time = 1.7 milliseconds, 3-D view

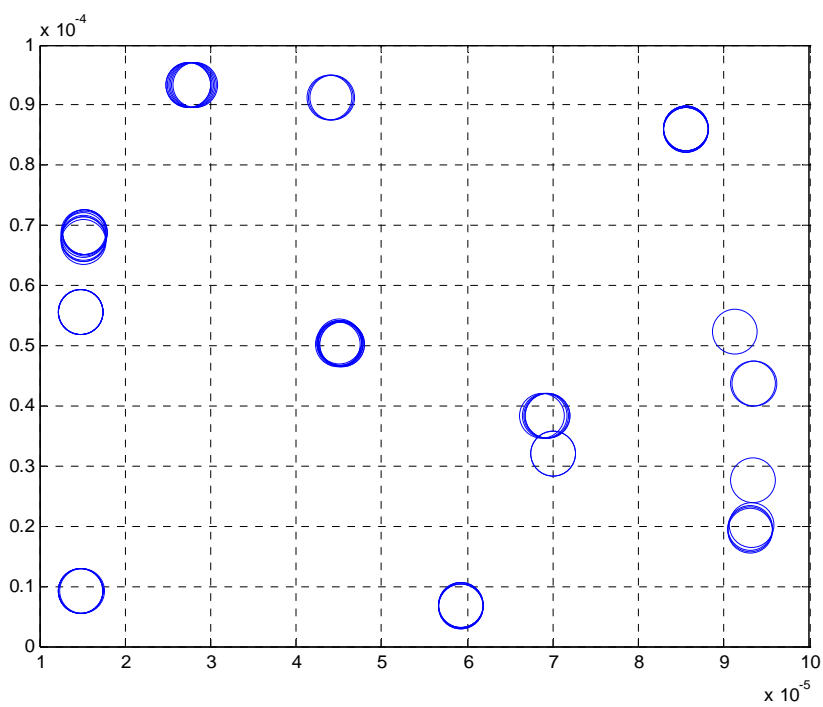


Figure 43. Simulation 6, Time = 1.7 milliseconds, Top Down View

Qualitatively, from the above figures, it is apparent that the speed in which the particles form chains is a function of the strength of the applied magnetic field. Examining the two extreme cases (Simulations 4 and 6) it is clear that the structures are much closer to completion in Figure 40 than those in Figure 28 (both are 0.86 milliseconds into the simulation). This result is intuitive based on the fact that the strength of the dipole force is proportional to the square of the applied magnetic field strength (Equations 1 and 3).

## B. DYNAMIC FLUID SIMULATION

The dynamic fluid simulation is where the real use for the MR model is realized. Most MR applications in industry use the MR effect on a moving fluid. It is desirable for the dynamic model to be able to accurately predict the microstructures of the particles in the MR fluid and from there predict the apparent viscosity and shear stress of the MR fluid. One theory for predicting the shear stress has already been developed and makes its predictions based on the chain density in the MR fluid and the angles the chains make in relation to the moving fluid [9].

A simulation of a MR fluid in shear was run in order to show that these measurements could be made in order to test the model against experimental evidence and to use the model to help design MR fluid devices. The simulation results are shown below and the following parameters were used.

	Number of Particles	Fluid Viscosity	Fluid Permeability	Particle Permeability	Applied Magnetic Field	Velocity of Top Plate
Simulation 7	40	.25 Pa s	1.26E-6 N/A <sup>2</sup>	.00377 N/A <sup>2</sup>	250 kA/m	0.1 m/s

Table 3. Parameters for Simulation 7

The following figures show the distribution of particles and their orientation in a dynamic flow. The dimensions for the area were changed in order to create a higher particle density without adding more particles to the volume. In this case the size of the

rectangular volume is 50 X 100 X 50 micrometers with the longer direction in the direction of the fluid velocity. The particles were only seeded in the left half of the volume to allow the fluid to push the particles to the right without interference from the wall. The magnetic field is applied in the negative z direction. The value of  $m/D$  used to calculate the time step has a value of 1.744E-7 as was the case for the above simulations.

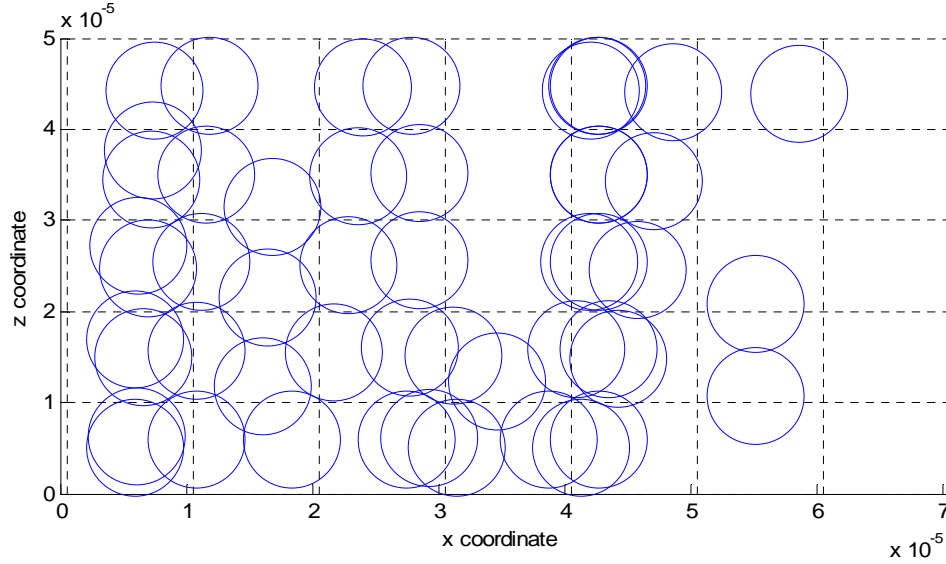


Figure 44. Side View of a MR Fluid in Shear

In the above figure the fluid is flowing from the left to the right based on the shear force developed due to the top plate moving to the left at 0.1 m/s. The angle that the chains make with relation to the fluid vary, but could easily be measured and averaged. Examining the top down view of the fluid shown below, would allow for the determination of the chain density.

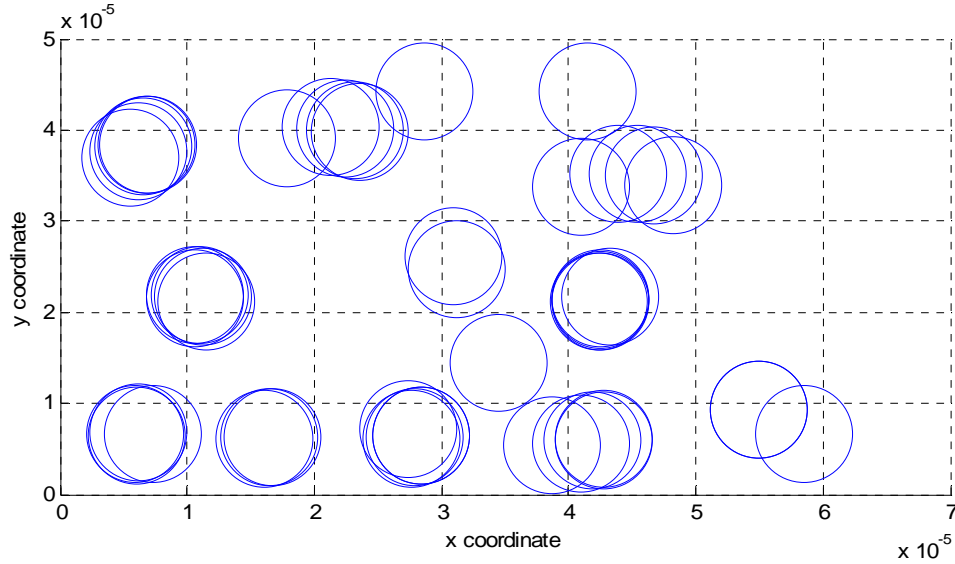


Figure 45. Top View of the MR Fluid in Shear

The dynamic model allows the user to easily input common variable parameters in a program in order to determine the dynamic microstructure in two common flow conditions (linear flow from shear and parabolic flow from a pressure gradient). For other, more permanent parameters (particle or fluid magnetic permeability, fluid viscosity, etc.) individual lines of code which set these parameters must be altered. For a more detailed description of what parameters the user inputs when running the code and other parameters directly set in the code see Appendix B.

The pressure driven, parabolic velocity profile fluid simulation is shown below. Unfortunately it is harder to determine the microstructure, in this case than for the shear case. The red line inserted on the below figures shows one chain and how it bulges in the middle based on the higher flow velocity there. The parameters for this simulation are exactly the same as those shown in Table 3, except the flow velocity is the centerline flow, not the flow at the top wall.

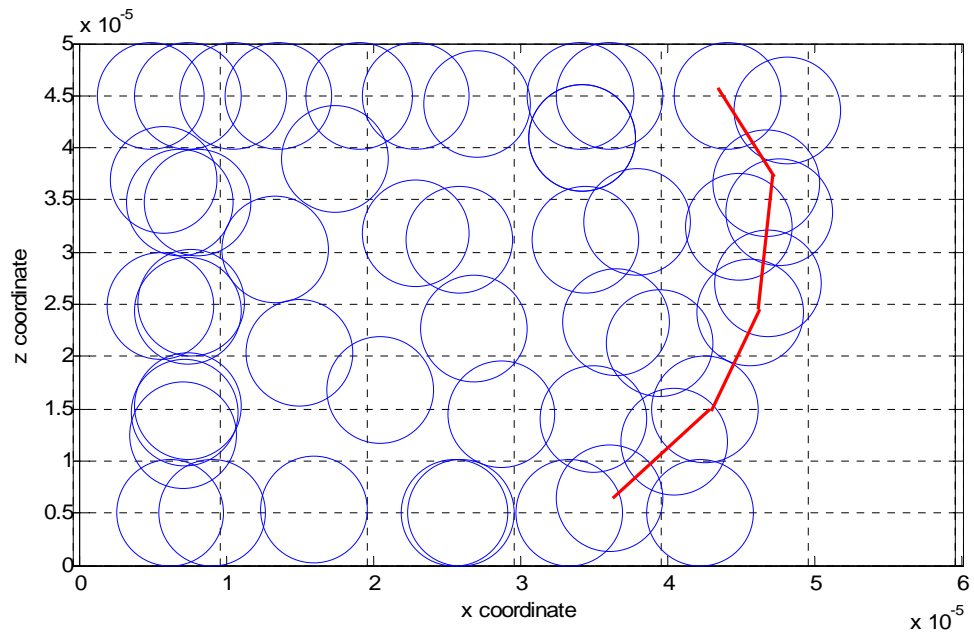


Figure 46. Side View of MR Fluid with Parabolic Flow

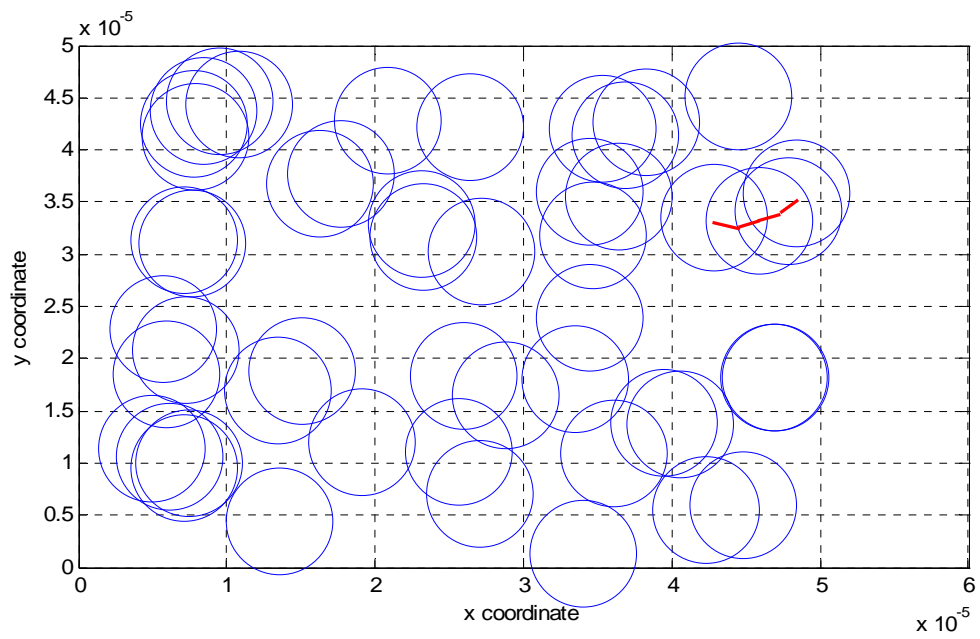


Figure 47. Top Down View of MR Fluid with Parabolic Flow

## VI. CONCLUSION

The goal of the model developed was for it to be simple, easy to use, require little empirical data (based on first principles) and be accurate. The model satisfies the requirement to be simple. It uses very well understood laws (Newton's Second Law, dipole interaction force, and Stokes' drag) to describe the forces and accelerations of the particles. Through a mathematical justification it ignores the inertial mass of the particles (being dominated by the viscous forces) to simplify the calculations even further. The physical interaction between the particles and the walls was chosen to be in a form that would balance out the other dominant forces in a way that was short ranged. This technique is also commonly used in other similar types of models.

The programs were written in order allow multiple simulations with a minimum amount of work. Instead of the user having to laboriously input every parameter required for every simulation the programs only require the user to input a small number of parameters that were assumed to be the most varied. The disadvantage to this approach is that the user must modify the code in order to change parameters such as particle or fluid magnetic permeability, fluid viscosity, or particle size. However, it was assumed that these parameters would not be changed as frequently as the magnetic field strength, size of the volume, or number of particles, so they were not requested by the program for every simulation.

The model used is based entirely on first principles so no empirical data is required for the simulation of particles. This could change if the model requires modification in order to accurately predict experimental results. For instance, in some regimes, the Stokes' approximation may no longer be valid. In this case the model should be modified to more accurately describe the shear and pressure forces on a submerged body and this may have to be done with empirical data. It is the hope and belief that this will not be required, but it is a possibility.

As far as accuracy is concerned the best way to check the model is against carefully controlled laboratory experiments. Qualitatively the model matches observed



data such as the chain formation and the time scale in which these structures form 10. However, there are several assumptions made that may have to be modified. The first assumption that limits the applicability of the dynamic model is the characterization of the velocity profile. In reality, the formation of particle chains alters the imposed flow. This is how MR fluids are able to withstand a shear and alter the bulk viscosity of the fluid. The model presented does not allow for the changing of the velocity profile. This is not a simple problem to solve, because the only way to determine how the flow changes based on the particle formations and how the particle formations vary based on the flow is to numerically solve to sets of equations simultaneously. Either Euler's equations or the Navier-Stokes' equations must be solved at each time step along with the other equations to determine the forces acting on the particles. This would require the integration of the model for the dynamic behavior of the magnetic particles with a numerical solver for fluid dynamic. The location of the particles at each time step would represent a boundary in the flow that would be solved with a flow solver. The model presented here does not attempt to perform any type of alteration of the flow based on the particle dynamics. Therefore, the model is not good for long simulation times, but it is still valid in the short term (before the initial velocity of the fluid is altered). In other words, this model accurately describes the initial particle dynamics, but is poor in the limit where the initial flow velocity would have been modified by the particle structures.

Another area requiring more detailed study is in the interaction between the particle chains and the magnet providing the magnetic field. As discussed earlier, this interaction is well understood in the ER case, but not for the MR. Models for ER fluid accurately describe, based on the interaction with the chains and the electrode, how particle chains will merge to form even larger structures around one second after the field is applied. These larger structures are also observed in MR fluids, but the method in which they form is being debated. Since it is doubted that the chains interact with the magnet in the same way that the ER fluid's chains interact with the electrodes, the same process is not occurring. Some have proposed that Brownian motion needs to be included. While the Brownian motion has much smaller interaction energy than magnetism, it is postulated that Brownian interaction could cause the chains to bulge and this temporary, minor change in position of the chain could allow for nearby chains to attract this chain. Again, this is a postulation, and more study is required for the particle-magnet interaction.

## APPENDIX A. DERIVATIONS OF EQUATION 4, 5, AND 6

Based on the figure below define  $\vec{f}_r$  as the component of  $\vec{f}_{ij}$  in the radial direction and  $\vec{f}_\theta$  as the component of  $\vec{f}_{ij}$  in the angular direction as shown.

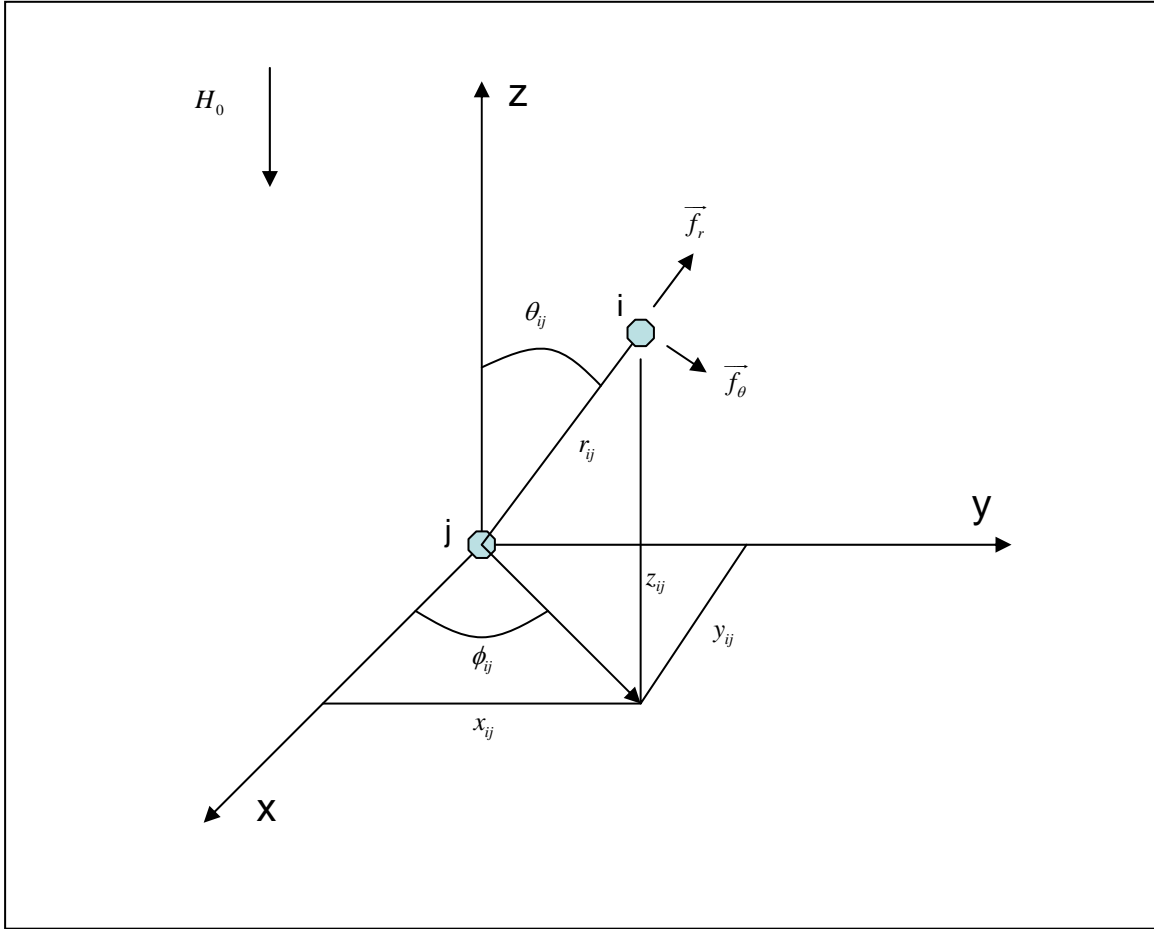


Figure 48. Geometrical Relationship Between Two Particles

After dropping the subscripts for convenience and decomposing  $\vec{f}_r$  into its Cartesian components gives

$$f_y = f_r \sin(\theta) \sin(\phi)$$

$$f_x = f_r \sin(\theta) \cos(\phi)$$

$$f_z = f_r \cos(\theta)$$

where  $f_y$ ,  $f_x$  and  $f_z$  are the magnitudes of the components of the force in the y, x and z directions respectively. Similar decompositions of  $\vec{f_\theta}$  into its Cartesian components gives

$$f_y = f_\theta \cos(\theta) \sin(\phi)$$

$$f_x = f_\theta \cos(\theta) \cos(\phi)$$

$$f_z = -f_\theta \sin(\theta)$$

with the same definitions as above. Adding the components together gives

$$f_y = f_r \sin(\theta) \sin(\phi) + f_\theta \cos(\theta) \sin(\phi)$$

$$f_x = f_r \sin(\theta) \cos(\phi) + f_\theta \cos(\theta) \cos(\phi)$$

$$f_z = f_r \cos(\theta) - f_\theta \sin(\theta).$$

Substituting the definition of  $f_\theta$  and  $f_\theta$  from equation (3) and the geometric identities

$$\sin(\theta) = \frac{\sqrt{x^2 + y^2}}{r}$$

$$\sin(\phi) = \frac{y}{\sqrt{x^2 + y^2}}$$

$$\cos(\theta) = \frac{z}{r}$$

$$\cos(\phi) = \frac{x}{\sqrt{x^2 + y^2}}$$

into the above equation obtains

$$f_y = \frac{Q}{r^4} \left[ 1 - \frac{5z^2}{r^2} \right] \frac{y}{r}$$

$$f_x = \frac{Q}{r^4} \left[ 1 - \frac{5z^2}{r^2} \right] \frac{x}{r}$$

$$f_z = \frac{Q}{r^4} \left[ 3 - \frac{5z^2}{r^2} \right] \frac{z}{r}$$

with  $Q = 3m^2\mu_f$ .

THIS PAGE INTENTIONALLY LEFT BLANK

## APPENDIX B. COMPUTER CODE AND DESCRIPTION

Below is the computer code for the computation of the static flow problem and a description of the various sections.

```
%Thesis program
clear all
a=5*10^-6; %m radius of particle
Vol=pi*a^3*4/3; %Volume of particle
mass=7850*Vol; %kg mass of particle

tf=input('Number of time steps ');
height=input('Height of volume (micro meter)');
height=height*10^-6; %converts to meters
length=input('Length of volume (micro meter)');
length=length*10^-6; %converts to meters
width=input('Width of volume (micro meter)');
width=width*10^-6;
N=input('Number of particles');
H=input('Magnetic Field intensity (kA/m)'); %~200 kA/m
H=H*1000;

xinit=length*rand(N,1); %initial x dist of particles
yinit=width*rand(N,1); %initial y dist of particles
zinit=height*rand(N,1); %initial z dist of particles

vis=.25; %fluid viscosity [Pa*s]
uf = 1.257E-6; %permeability of fluid
up = .00377; %permeability of particle
m = (4/3)*pi*H*a^3*(up-uf)/(up+2*uf); %magnetic moment
D=6*pi*vis*a; %Stokes drag force coefficient
tcheck=mass/D; %intrinsic time scale
Q = 3*m^2*uf;

ysys = zeros(tf,N); %y position of particles, column 1 refers to
particle 1, column 2 refers to particle 2, ect
xsys = zeros(tf,N); %x position of particles, column 1 refers to
particle 1, column 2 refers to particle 2, ect
zsys = zeros(tf,N); %z position of particles, column 1 refers to
particle 1, column 2 refers to particle 2, ect
delx = zeros(N,N); %difference in the x position between the particles
dely = zeros(N,N); %difference in the y position between the particles
delz = zeros(N,N); %difference in the z position between the particles
r=zeros(N,N);
Fmx=zeros(N,N);
Fmy=zeros(N,N);
Fpx=zeros(N,N);
Fpy=zeros(N,N);
Fpz=zeros(N,N);
```

```

Fmz=zeros(N,N);

ysys(1,:) = yinit';
xsys(1,:) = xinit';
zsys(1,:) = zinit';

for t = 1:tf
    x = xsys(t,:);
    y = ysys(t,:);
    z = zsys(t,:);
    for i=1:N
        for j=1:N
            delx(i,j) = x(i)-x(j);
            dely(i,j) = y(i)-y(j);
            delz(i,j) = z(i)-z(j);
            r(i,j) = sqrt(delx(i,j)^2+dely(i,j)^2+delz(i,j)^2);
            if i==j
                Fmx(i,j)=0;
                Fmy(i,j)=0;
                Fpy(i,j)=0;
                Fpx(i,j)=0;
                Fpz(i,j)=0;
                Fmz(i,j)=0;
            else
                Fmx(i,j)=-Q*delx(i,j)/r(i,j)^5*(5*(delz(i,j)/r(i,j))^2-
1); %force on particle i from particle j in x direction due to magnetic
force
                Fpx(i,j)=2*Q/((2*a)^4)*(delx(i,j)/(r(i,j)))*exp(-
12*((r(i,j)/(2*a))-1)); %force on particle i from particle j in x
direction due to physical interaction (collision)
                Fmy(i,j)=-Q*dely(i,j)/r(i,j)^5*(5*(delz(i,j)/r(i,j))^2-
1); %force on particle i from particle j in y direction due to magnetic
force
                Fpy(i,j)=2*Q/((2*a)^4)*(dely(i,j)/(r(i,j)))*exp(-
12*((r(i,j)/(2*a))-1)); %force on particle i from particle j in y
direction due to physical interaction (collision)
                Fmz(i,j)=-Q*delz(i,j)/r(i,j)^5*(5*(delz(i,j)/r(i,j))^2-
3);
                Fpz(i,j)=2*Q/((2*a)^4)*(delz(i,j)/(r(i,j)))*exp(-
12*((r(i,j)/(2*a))-1));
                Fx=Fmx+Fpx; %total force in x direction
                Fy=Fmy+Fpy; %total force in y direction
                Fz=Fmz+Fpz; %total force in z direction
            end
        end
    end
    Ftx=sum(Fx,2); %total force on each particle in x direction
    Fty=sum(Fy,2); %total force on each particle in y direction
    Ftz=sum(Fz,2); %total force on each particle in z direction
end
for q=1:N
    Ftz(q)=Ftz(q)+2*Q/((2*a)^4)*exp(-30*(z(q)/(2*a)-.5));
    Ftz(q)=Ftz(q)-2*Q/((2*a)^4)*exp(-30*((height-z(q))/(2*a)-
.5)); %loop incorporates force due to repulsion of wall
    Ftx(q)=Ftx(q)+2*Q/((2*a)^4)*exp(-30*(x(q)/(2*a)-.5));

```

```

        Ftx(q)=Ftx(q)-2*Q/((2*a)^4)*exp(-30*((length-x(q))/(2*a)-
.5));
        Fty(q)=Fty(q)+2*Q/((2*a)^4)*exp(-30*(y(q)/(2*a)-.5));
        Fty(q)=Fty(q)-2*Q/((2*a)^4)*exp(-30*((width-y(q))/(2*a)-
.5));
    end

    if t<10
        tau=tcheck/1E7;
    elseif t<100
        tau=tcheck/1E4;
    elseif t<1000
        tau=tcheck/1E2;
    else
        tau=tcheck/10;
    end

    xsys(t+1,:)=x+Ftx'*tau/D;
    ysys(t+1,:)=y+Fty'*tau/D;
    zsys(t+1,:)=z+Ftz'*tau/D;

    plot3(xsys(t+1,:),ysys(t+1,:),zsys(t+1,:), 'o', 'Markersize',25);

    axis ([0,length,0,width,0,height])
    pause(.0001)
end

```

The first section clears all currently stored variables, sets particle size and calculates the mass of the particles.

```

%Thesis program
clear all
a=5*10^-6; %m radius of particle
Vol=pi*a^3*4/3; %Volume of particle
mass=7850*Vol; %kg mass of particle

```

The next section is for the user to input the number of time steps, volume dimensions, number of particles, and magnetic field strength. It also converts these inputs into the proper units.

```

tf=input('Number of time steps ');
height=input('Height of volume (micro meter)');
height=height*10^-6; %converts to meters
length=input('Length of volume (micro meter)');
length=length*10^-6; %converts to meters
width=input('Width of volume (micro meter)');
width=width*10^-6;
N=input('Number of particles');
H=input('Magnetic Field intensity (kA/m)'); %~200 kA/m

```



```
H=H*1000;
```

The next section of code randomly decides the initial positions of the particles and stores them in the variables shown.

```
xinit=length*rand(N,1); %initial x dist of particles  
yinit=width*rand(N,1); %initial y dist of particles  
zinit=height*rand(N,1); %initial z dist of particles
```

The next section set some parameters of the MR fluid (magnetic permeability of the particle and fluid and fluid viscosity) and computes the magnetic dipole moment, Stokes' drag coefficient, and the intrinsic time scale (to be used in determining the actual time scale later in the program).

```
vis=.25; %fluid viscosity [Pa*s]  
uf = 1.257E-6; %permeability of fluid  
up = .00377; %permeability of particle  
m = (4/3)*pi*H*a^3*(up-uf)/(up+2*uf); %magnetic moment  
D=6*pi*vis*a; %Stokes drag force coefficient  
tcheck=mass/D; %intrinsic time scale  
Q = 3*m^2*uf;
```

The next section preallocates memory for the matrices that will be used to either store or compute the motion of the particles. The matrices *xsys*, *ysys*, and *zsys* will store the actual positions of the particles. The columns refer to the individual particles (the first column is the position of particle 1, the second column refers to the position of particle 2, etc.) and the rows refer to the time (the first row is the initial distribution, the second row is the position of the particles after one time step, etc.). The matrices *delx*, *dely* and *delz* temporarily store the differences in the x, y and z direction between particles. The index of the matrix determines the difference in position of which particles. For example, *delx*(4,9) is the difference in the x position between particles 4 and 9. These matrices get written over after each time step. The matrix *r* is similar to *delx*, *dely* and *delz* but stores the difference in the radial direction between particles. The matrices *Fmx*, *Fmy*, and *Fmz* store the x, y and z components of the force between two particles due to their magnetic dipoles. For example, *Fmy*(2,6) is the dipole force in the y direction between particles 2 and 6. *Fpx*, *Fpy*, and *Fpz* are similar to *Fmx*, *Fmy*, and *Fmz*

except that the former relate to the physical repulsive force due to the particles being hard spheres.

```
ysys = zeros(tf,N); %y position of particles, column 1 refers to
particle 1, column 2 refers to particle 2, ect
xsys = zeros(tf,N); %x position of particles, column 1 refers to
particle 1, column 2 refers to particle 2, ect
zsys = zeros(tf,N); %z position of particles, column 1 refers to
particle 1, column 2 refers to particle 2, ect
delx = zeros(N,N); %difference in the x position between the particles
dely = zeros(N,N); %difference in the y position between the particles
delz = zeros(N,N); %difference in the z position between the particles
r=zeros(N,N);
Fmx=zeros(N,N);
Fmy=zeros(N,N);
Fmz=zeros(N,N);
Fpx=zeros(N,N);
Fpy=zeros(N,N);
Fpz=zeros(N,N);
```

The next section takes the initial particle distribution and stores this data in the first row of the corresponding position matrices.

```
ysys(1,:) = yinit';
xsys(1,:) = xinit';
zsys(1,:) = zinit';
```

The next section is the heart of the program that calculates the dipole and physical interaction between particles. These nested loops calculate first the *delx*, *dely*, *delz* and *r* matrices for the current time step. Then set the diagonal elements of the force matrices to zero (a particle does not interact with itself). It then uses the equations discussed in the thesis to calculate all of the other elements in the force matrices.

```
for t = 1:tf
    x = xsys(t,:);
    y = ysys(t,:);
    z = zsys(t,:);
    for i=1:N
        for j=1:N
            delx(i,j) = x(i)-x(j);
            dely(i,j) = y(i)-y(j);
            delz(i,j) = z(i)-z(j);
            r(i,j) = sqrt(delx(i,j)^2+dely(i,j)^2+delz(i,j)^2);
            if i==j
                Fmx(i,j)=0;
                Fmy(i,j)=0;
                Fpy(i,j)=0;
```

```

        Fpx(i,j)=0;
        Fpz(i,j)=0;
        Fmz(i,j)=0;
    else
        Fmx(i,j)=-Q*delx(i,j)/r(i,j)^5*(5*(delz(i,j)/r(i,j))^2-
1); %force on particle i from particle j in x direction due to magnetic
force
        Fpx(i,j)=2*Q/((2*a)^4)*(delx(i,j)/(r(i,j)))*exp(-
12*((r(i,j)/(2*a))-1)); %force on particle i from particle j in x
direction due to physical interaction (collision)
        Fmy(i,j)=-Q*dely(i,j)/r(i,j)^5*(5*(delz(i,j)/r(i,j))^2-
1); %force on particle i from particle j in y direction due to magnetic
force
        Fpy(i,j)=2*Q/((2*a)^4)*(dely(i,j)/(r(i,j)))*exp(-
12*((r(i,j)/(2*a))-1)); %force on particle i from particle j in y
direction due to physical interaction (collision)
        Fmz(i,j)=-Q*delz(i,j)/r(i,j)^5*(5*(delz(i,j)/r(i,j))^2-
3);
        Fpz(i,j)=2*Q/((2*a)^4)*(delz(i,j)/(r(i,j)))*exp(-
12*((r(i,j)/(2*a))-1));
        Fx=Fmx+Fpx; %total force in x direction
        Fy=Fmy+Fpy; %total force in y direction
        Fz=Fmz+Fpz; %total force in z direction
    end

    end

    Ftx=sum(Fx,2); %total force on each particle in x direction
    Fty=sum(Fy,2); %total force on each particle in y direction
    Ftz=sum(Fz,2); %total force on each particle in z direction
end

```

The next section incorporates a loop to add the force due to the physical interaction with the wall.

```

for q=1:N
    Ftz(q)=Ftz(q)+2*Q/((2*a)^4)*exp(-30*(z(q)/(2*a)-.5));
    Ftz(q)=Ftz(q)-2*Q/((2*a)^4)*exp(-30*((height-z(q))/(2*a)-.5));
%loop incorporates force due to repulsion of wall
    Ftx(q)=Ftx(q)+2*Q/((2*a)^4)*exp(-30*(x(q)/(2*a)-.5));
    Ftx(q)=Ftx(q)-2*Q/((2*a)^4)*exp(-30*((length-x(q))/(2*a)-.5));
    Fty(q)=Fty(q)+2*Q/((2*a)^4)*exp(-30*(y(q)/(2*a)-.5));
    Fty(q)=Fty(q)-2*Q/((2*a)^4)*exp(-30*((width-y(q))/(2*a)-.5));
end

```

The next section uses the intrinsic time scale to create an actual time scale based on the time that the program is simulating. Extremely small time scales are used initially to allow the initial structures to begin forming and then the time scales are enlarged as the structures become closer to equilibrium.

```

if t<10
    tau=tcheck/1E7;
elseif t<100
    tau=tcheck/1E4;
elseif t<1000
    tau=tcheck/1E2;
else
    tau=tcheck/10;
end

```

The final section calculates the new position of every particle, stores it in the appropriate matrices and plots the positions on a 3-D graph.

```

xsys(t+1,:)=x+Ftx'*tau/D;
ysys(t+1,:)=y+Fty'*tau/D;
zsys(t+1,:)=z+Ftz'*tau/D;

plot3(xsys(t+1,:),ysys(t+1,:),zsys(t+1,:), 'o', 'Markersize',25);

axis ([0,length,0,width,0,height])
pause(.0001)

```

Below is the attached code for the shear flow problem. This code is very similar to the static code above, except for a few lines described. Sentences in red are the descriptions of the changes and do not appear in the code.

```

%Thesis program
clear all
a=5*10^-6; %m radius of particle
Vol=pi*a^3*4/3; %Volume of particle
mass=7850*Vol; %kg mass of particle

tf=input('Number of time steps ');
height=input('Height of volume (micro meter)');
height=height*10^-6; %converts to meters
length=input('Length of volume (micro meter)');
length=length*10^-6; %converts to meters
width=input('Width of volume (micro meter)');
width=width*10^-6;
U=input('Velocity of top plate (m/s)'); User inputs the velocity of
the top plate
N=input('Number of particles');
H=input('Magnetic Field intensity (kA/m)'); %~200 kA/m
H=H*1000;

xinit=length*rand(N,1); %initial x dist of particles
yinit=width*rand(N,1); %initial y dist of particles
zinit=height*rand(N,1);

```

```

vis=.25;
uf = 1.257E-6; %permeability of fluid
up = .00377; %permeability of particle

m = 4*pi*H*a^3*(up-uf)/(up+2*uf); %magnetic moment, may to modify H
since local magnetic field may not be applied field (see paper
micromechanical model for MR fluids)
D=6*pi*vis*a; %Stokes drag force coefficient
tcheck=mass/D; %intrinsic time scale
Q = 3*m^2*uf;

ysys = zeros(tf,N); %y position of particles, column 1 refers to
particle 1, column 2 refers to particle 2, ect
xsys = zeros(tf,N); %x position of particles, column 1 refers to
particle 1, column 2 refers to particle 2, ect
zsys = zeros(tf,N);
delx = zeros(N,N);
dely = zeros(N,N);
delz = zeros(N,N);
r=zeros(N,N);

Fmx=zeros(N,N);
Fmy=zeros(N,N);
Fpx=zeros(N,N);
Fpy=zeros(N,N);
Fpz=zeros(N,N);
Fmz=zeros(N,N);

ysys(1,:) = yinit';
xsys(1,:) = xinit';
zsys(1,:) = zinit';

for t = 1:tf
    x = xsys(t,:);
    y = ysys(t,:);
    z = zsys(t,:);
    for i=1:N
        for j=1:N
            delx(i,j) = x(i)-x(j);
            dely(i,j) = y(i)-y(j);
            delz(i,j) = z(i)-z(j);
            r(i,j) = sqrt(delx(i,j)^2+dely(i,j)^2+delz(i,j)^2);
            if i==j
                Fmx(i,j)=0;
                Fmy(i,j)=0;
                Fpy(i,j)=0;
                Fpx(i,j)=0;
                Fpz(i,j)=0;
                Fmz(i,j)=0;
            else
                Fmx(i,j)=-Q*delx(i,j)/r(i,j)^5*(5*(delz(i,j)/r(i,j))^2-
1); %force on particle i from particle j in x direction due to magnetic
force

```

```

        Fpx(i,j)=Q/((2*a)^4)*(delx(i,j)/(r(i,j)))*exp(-
12*((r(i,j)/(2*a))-1)); %force on particle i from particle j in x
direction due to physical interaction (collision)
        Fmy(i,j)=-Q*dely(i,j)/r(i,j)^5*(5*(delz(i,j)/r(i,j))^2-
1); %force on particle i from particle j in y direction due to magnetic
force
        Fpy(i,j)=Q/((2*a)^4)*(dely(i,j)/(r(i,j)))*exp(-
12*((r(i,j)/(2*a))-1)); %force on particle i from particle j in y
direction due to physical interaction (collision)
        Fmz(i,j)=-Q*delz(i,j)/r(i,j)^5*(5*(delz(i,j)/r(i,j))^2-
3);
        Fpz(i,j)=2*Q/((2*a)^4)*(delz(i,j)/(r(i,j)))*exp(-
12*((r(i,j)/(2*a))-1));
        Fx=Fmx+Fpx; %total force in x direction
        Fy=Fmy+Fpy; %total force in y direction
        Fz=Fmz+Fpz;
    end

    end

    Ftx=sum(Fx,2); %total force on each particle in x direction
    Fty=sum(Fy,2); %total force on each particle in y direction
    Ftz=sum(Fz,2); %total force on each particle in z direction
end
for q=1:N
    if z(q)<1.2*a && z(q)>= a
        Ftx(q)=0;
        Fty(q)=0;
        Ftz(q)=0;
    else
        Ftz(q)=Ftz(q)+2*Q/((2*a)^4)*exp(-30*(z(q)/(2*a)-.5));
        Ftz(q)=Ftz(q)-2*Q/((2*a)^4)*exp(-30*((height-z(q))/(2*a)-
.5)); %loop incorporates force due to repulsion of wall
        Ftx(q)=Ftx(q)+2*Q/((2*a)^4)*exp(-30*(x(q)/(2*a)-.5));
        Ftx(q)=Ftx(q)-2*Q/((2*a)^4)*exp(-30*((length-x(q))/(2*a)-
.5));
        Ftx(q)=Ftx(q)+D*U*(z(q)-a)/height; This line adds the force
on the particle in the x direction due to the moving fluid. The force
is assumed linear (zero at the bottom and maximum at the top).
        Fty(q)=Fty(q)+2*Q/((2*a)^4)*exp(-30*(y(q)/(2*a)-.5));
        Fty(q)=Fty(q)-2*Q/((2*a)^4)*exp(-30*((width-y(q))/(2*a)-
.5));
    end
end

if t<10
    tau=tcheck/1E7;
elseif t<100
    tau=tcheck/1E5;
elseif t<1000
    tau=tcheck/1E3;
else
    tau=tcheck/100;
end
end

```

```

    xsys(t+1,:)=x+Ftx'*tau/D;
    ysys(t+1,:)=y+Fty'*tau/D;
    zsys(t+1,:)=z+Ftz'*tau/D;

    plot3(xsys(t+1,:),ysys(t+1,:),zsys(t+1,:), 'o', 'Markersize',25);

    axis ([0,length,0,width,0,height])
    pause(.0001)
end

```

## LIST OF REFERENCES

- [1] S. Genç and P. Phule, "Rheological Properties of Magnetorheological Fluids," *Journal of Smart Materials and Structures*, vol. 11, pp. 140-146, Feb 2002.
- [2] Rabinow, J., "Magnetic Fluid Torque and Force Transmitting Device," U.S. Patent 2,575,360, Nov 20, 1951.
- [3] H. V. Ly, F. Reitich, M. R. Jolly, H. T. Banks, and K. Ito, "Simulations of Particle Dynamics in Magnetorheological Fluids," *Journal of Computational Physics*, vol. 155, pp. 160-177, June 1999.
- [4] R. Tao, "Super-strong Magnetorheological Fluids," *Journal of Physics: Condensed Matter*, vol. 13, pp. 979-999, Nov 2001.
- [5] W. R. Smythe, *Static and Dynamic Electricity*, 3<sup>rd</sup> ed. McGraw-Hill, 1968, pp. 350-352.
- [6] Jing Liu, E. M. Lawrence, A. Wu, M. L. Ivey, G. A. Flores, K. Javier, J. Bibett, and J. Richard, "Field-Induced Structures in Ferrofluid Emulsions," *Physics Review Letter*, vol. 74, p. 2828, Apr 1995.
- [7] M. Mohebi, N. Jamasbi and Jing Liu, "Simulation of the Formation of Nonequilibrium Structures in Magnetorheological Fluids Subject to an External Magnetic Field," *Physics Review. E*, vol. 54, Nov 1996.
- [8] W. Panofsky and M. Phillips, *Classical Electricity and Magnetism*, 2<sup>nd</sup> ed. Addison-Wesley Publishing Company Inc., 1962, pp. 144-145.
- [9] H. Si, X. Peng and X. Li, "A Micromechanical Model for Magnetorheological Fluids," *Journal of Intelligent Materials and Structures*, vol. 19, pp. 19-23, Feb 2007.
- [10] Lord Corporation, "Technology Compared," <http://www.lord.com/Home/MagnetoRheologicalMRFluid/MRFluidTechnology/TechnologyCompared/tabid/3773/Default.aspx>, accessed June 2008.



THIS PAGE INTENTIONALLY LEFT BLANK

## **INITIAL DISTRIBUTION LIST**

1. Defense Technical Information Center  
Ft. Belvoir, Virginia
2. Dudley Knox Library  
Naval Postgraduate School  
Monterey, California
3. Mechanical Engineering Department Chair, Code ME  
Distinguished Professor Anthony J. Healey  
Naval Postgraduate School  
Monterey, California
4. Professor John Lloyd  
Naval Postgraduate School  
Monterey, California
5. LT Joseph Spinks  
Naval Submarine Base New London  
Groton, Connecticut